**Title**
Improving Operations Using Advanced Surveillance Metrics and Existing Traffic Detectors



**Authors**
Coifman, Benjamin
Varaiya, Pravin

**Publication Date**
2002

CALIFORNIA PATH PROGRAM
INSTITUTE OF TRANSPORTATION STUDIES
UNIVERSITY OF CALIFORNIA, BERKELEY

# Improving Operations Using Advanced Surveillance Metrics and Existing Traffic Detectors

**Benjamin Coifman**
**Pravin Varaiya**

**California PATH Research Report**
**UCB-ITS-PRR-2002-2**

This work was performed as part of the California PATH Program of the University of California, in cooperation with the State of California Business, Transportation, and Housing Agency, Department of Transportation; and the United States Department of Transportation, Federal Highway Administration.



Final Report for MOU 3010

January 2002

ISSN 1055-1425

# Improving Operations Using Advanced Surveillance Metrics and Existing Traffic Detectors.

MOU 3010 Final Report

Dr. Benjamin Coifman
Civil Engineering
470 Hitchcock Hall
The Ohio State University
Columbus, OH 43210
V: (614) 292-4282
F: (614) 292-3780
E: Coifman.1@OSU.edu

Professor Pravin Varaiya
University of California, Berkeley
Department of Electrical Engineering and Computer Science
271M Cory Hall
Berkeley, CA 94720-1770
V: (510) 642-0348
F: (510) 642-6330
E: varaiya@eecs.berkeley.edu

# 1 OVERVIEW

Because travel time provides information over an extended freeway link, rather than at a single point, it is a key parameter for ATIS applications and it is a powerful tool for ATMS. Under PATH sponsorship, we have already developed a prototype travel time measurement system that utilizes existing dual loop speed traps and "model 170" controllers. This research has advanced the work by improving the vehicle reidentification algorithms (Sections 2 and 3) and applying the travel time measurement system over seven freeway links in real-time (Section 4). This latter work was conducted as part of the Berkeley Highway Laboratory (BHL). The detector data are passed on to Caltrans District 4 operations and archived for subsequent research. In addition to the previous work, which uses data from two or more detector stations to measure travel time, we have conducted a pilot study to estimate link travel time using data from a single detector station. The estimation work was conducted in conjunction with MOU 3000 and the results are presented in *Traffic Data Measurement and Validation, MOU 3000 Final Report.*

# 2 VEHICLE REIDENTIFICATION AND TRAVEL TIME MEASUREMENT, PART I: CONGESTED FREEWAYS[1]

## *2.1 Introduction*

This Section presents a vehicle reidentification algorithm for consecutive detector stations on a freeway, whereby a vehicle measurement made at a downstream detector station is matched with the vehicle's corresponding measurement at an upstream station. The work should be applicable to any detector technology capable of extracting a reproducible vehicle measurement, or *vehicle signature*. For the present research, the algorithm uses the effective vehicle lengths measured by conventional dual-loop-detectors.[2] As such, the algorithm can be deployed without requiring new detector hardware. The length measurements, however, may only be accurate to two feet (or worse) due to the resolution limitations of dual-loop-detector data.

For a given vehicle measurement at the downstream detector station, the algorithm uses arrival times and number of arrivals at the detector to identify the set of all upstream observations in the same lane that could have come from the same vehicle. The measurement resolution makes it difficult to identify which one of these measurements, if any of them, correspond to the downstream vehicle. To address this limitation, the algorithm takes the difference between the downstream measurement and each of the upstream measurements. It then identifies all pairs whose difference exceeds the measurement accuracy. These measurements presumably could not have come from the same vehicle, while all remaining pair-wise comparisons are treated as possible matches. Of course, with this simple test, the downstream vehicle will likely have many possible matches within the set. We term the collection of incorrect matches as false positives. Toward eliminating the false positives, the algorithm uses a remarkably simple yet very effective technique: it matches platooned vehicles whenever these pass both the upstream and downstream detector stations without altering their relative sequence. The sequence of a platoon's vehicle lengths provides more information than do the individual measurements, as is demonstrated herein.

For reasons that will be discussed in this Section, the accuracy of a dual-loop-detector's vehicle length measurement improves as vehicle velocity decreases. Consequently, for the existing detectors, the algorithm is limited to matching vehicles during congested traffic conditions, i.e., when the local velocity measured by the detectors is less than 45 mph at one or both of the stations.

---

[1] M. Cassidy helped prepare this Section.

[2] The effective vehicle length is the length as "seen" by the detectors; i.e., the sum of the physical vehicle length and the length of the detection zone.

This limitation is not problematic, since freely flowing traffic is characterized by relatively constant velocities and thus, travel times can be estimated from the local conditions at the detector stations. To address this problem, Section 3 presents an algorithm for measuring travel time from dual-loop-detectors during free flow traffic conditions.

The travel time data recorded from the algorithm have a number of potential applications. For example, these data might improve traffic management tasks such as automatic incident detection, adaptive freeway ramp control, and traveler information systems. The data might also be used for routing vehicles over a network so as to reduce traveler delay, for calibrating traffic planning and simulation models, and for quantifying the potential benefits of emerging detector technologies that extract more detailed information from individual vehicles. Further discussion on potential applications can be found in Coifman (1998a).

The following Subsection provides a brief review of previous work related to automatic vehicle reidentification and in emerging technologies that might enhance this task. Next, the vehicle reidentification algorithm is presented in detail, using field-measured freeway data to illustrate the various steps. The Section closes with a brief discussion regarding possible future work in this area.

### *2.2 Previous Research*

Although at present, the proposed algorithm is used to match length measurements made by conventional dual-loop-detectors, the algorithm could be applied to vehicle signatures from other detector technologies. By providing improved measurement accuracy, these technologies might be used with our algorithm for improving the reidentification process. Examples of such signatures and their associated technologies include (1) inductive vehicle signatures collected from loop detectors using new sensor hardware (e.g., Kühne et al., 1997); (2) visual vehicle signatures from wayside cameras (e.g., MacCarley, 1998); (3) vehicle dimensions from laser detectors (e.g., Larson et al., 1998). Notably, some of the above technologies have been designed to measure vehicle dimensions, such as length, with an error less than one inch even when the vehicles are traveling at free flow speeds.

These new detector technologies have been expressly developed for vehicle reidentification applications. Likewise, several algorithms have been proposed for measuring travel time directly using the improved vehicle signatures (e.g., Reijmers, 1979, Pfannerstill, 1984, Kühne and Immes, 1993, Huang and Russell, 1997). The implementation of the aforementioned algorithms, however, requires the deployment of new detector hardware, even before the benefits of measuring

travel time can be quantified. Consequently, most installations of these systems have been limited to small test sites.

Of course, automatic vehicle identification (AVI) systems that rely on machine readable identification tags have also been deployed (e.g., Levine and McCasland, 1994, Balke et al., 1995, Cui and Huang, 1997). These systems provide reliable travel time measurements. However, the AVI systems do not monitor local conditions at the detector stations (such as flow, velocity and occupancy), this omission can impact traffic surveillance and control.

Other surveillance systems have been proposed for estimating vehicle travel time from aggregate traffic parameters like occupancy (e.g., Dailey, 1993, Petty et al., 1997). Although promising for free flow and lightly congested conditions, these systems can estimate travel time within seven percent accuracy during congestion (Petty et al., 1997). Another approach for estimating travel time is to match vehicles simply based on the cumulative arrivals at successive detector stations, i.e., the n-th vehicle at one station is matched to the n-th vehicle at the next station (e.g., Westerman and Immers, 1992, Westerman et al., 1996). To counter detector drift between stations, these systems use aggregate measurements to recalibrate during free flow conditions. Unfortunately, congestion can last several hours, leading to significant measurement drift between recalibrations. Finally, the vehicle reidentification algorithm discussed in this Section is an extension of simpler algorithms previously presented in Coifman (1998b).

### *2.3 The Proposed Algorithm*

The vehicle reidentification algorithm is described here via its application; i.e., it is applied to traffic data measured at two neighboring dual-loop-detector stations in a single travel lane along eastbound Interstate 80 in Berkeley, California. The site is shown in Figure 2-1. Video data were collected at each station and all vehicles that passed during the study period were visually matched between the two locations. Thus, the travel times extracted by the algorithm could be verified. Over 1,300 vehicles passed both stations in the subject lane during the video taping, while another 200 vehicles entered or exited the subject lane between the stations.

We begin this Subsection by briefly reviewing how a dual-loop-detector can be used to measure vehicle lengths. To this end, Figure 2-2A shows a time-space diagram depicting a vehicle passing over a dual-loop-detector. The controller normally records four transitions, i.e., the turn-on and turn-off times at each of the loops, as shown in Figure 2-2B. Occasionally a vehicle will change lanes over the dual-loop-detector or one of the loops malfunctions. In the event of such a detection error, only one loop will record the vehicle. These events are identified and discarded following

the method presented in Coifman (1998a). To the algorithm, any discarded vehicle will simply appear to be a vehicle that entered or exited the lane between the stations. The algorithm addresses these *phantom lane change maneuvers* in the same fashion that it addresses actual lane change maneuvers, as presented in a subsequent Subsection.

After accounting for detection errors, the following parameters are calculated for each vehicle: dual loop traversal time via the rising edges, $TT_r$, dual loop traversal time via the falling edges, $TT_f$, total on-time at the first loop, $OT_1$, and total on-time at the second loop, $OT_2$, as shown in Figure 2-2A. Obviously, the loop separation (20 ft in this case) divided by the traversal time yields the vehicle velocity. It is clear from Figure 2-2A that two measurements are available for the effective vehicle length,

$$\text{length measurement \#1:} \quad L_1 = 20 \cdot \frac{OT_1}{TT_r} \quad [\text{ft}] \tag{2-1}$$

$$\text{length measurement \#2:} \quad L_2 = 20 \cdot \frac{OT_2}{TT_f} \quad [\text{ft}]$$

and the algorithm uses the average of the two.

Notably, the controller samples the loops at 60 Hz, so at best, the traversal times and on-times in Equation 2-1 are accurate to 1/60 sec. To capture this resolution constraint, the measurement uncertainty is defined as the range spanned by $L_1$ and $L_2$ after including ±1/60 sec in $OT_1$, $OT_2$, $TT_r$ and $TT_f$. By inspection of Equation 2-1 and Figure 2-2A, this measurement uncertainty range is inversely proportional both to velocity and to the true vehicle length. Misdetections will impact the calculation, e.g., if one of the on-times was too short due to a detection error. Depending on the severity, such errors might not impact the algorithm, but if they do, they will simply appear to be phantom lane change maneuvers. To ensure the accuracy of $OT_1$, $OT_2$, $TT_r$ and $TT_f$, any hardware problems at each station, such as cross talk between detectors, were identified using Coifman (1999) and corrected.

### 2.3.1 Vehicle Arrival Numbers and Possible Matches

First, in the subject lane, vehicles are assigned consecutive arrival numbers as they pass each detector station and these numbers are assigned independently at each station. Next, a *set of feasible upstream measurements* is identified for each vehicle measured downstream. Assuming that the downstream vehicle did not change lanes between detector stations, the set should be chosen to ensure the true match for the vehicle falls within the set while not being so large as to

preclude a computer from processing the data. For this document, the set was defined as the most recent 100 measurements at the upstream detector prior to the downstream measurements. The size was chosen somewhat arbitrarily but subsequently verified to be adequate. In practice, a conservative set size could be estimated from the subject lane's jam density storage between the two detector stations.

Because a given vehicle length is not unique and because of the aforementioned measurement errors caused by the detector, it is not possible to match directly upstream and downstream measurements. To illustrate this point, Figure 2-3A shows a sequence of upstream length measurements with dark rectangles. The measurements are plotted in the order that the vehicles were observed at the upstream station. The vehicle lengths corresponding to each data point are shown by their positions along the ordinate, including the measurement uncertainty. For simplicity all of the vehicles are shown with the same uncertainty, but in practice, the range depends on the measurements and it varies from one vehicle to the next.

A single measurement made at the downstream station, along with its measurement uncertainty, is superimposed as a long, lightly shaded rectangle on Figure 2-3A. One observes a number of measurements from the upstream station that might correspond to the vehicle measured downstream; i.e., a number of lengths measured among the former coincide with the latter. These possible matches are indicated with open circles in Figure 2-3B. The algorithm eliminates from further consideration the upstream measurements that do not coincide with the downstream one.

### 2.3.2 Possible Matches and Sequences

A sequence of measured vehicle lengths (e.g., from a platoon) rapidly becomes distinct and the sequences measured at an upstream detector station can often be reidentified at a downstream station. Thus, the algorithm searches for sequences of measured vehicle lengths in the subject lane that exhibit strong correlation across the two detector stations. Since lane changes and measurement errors disrupt the sequences, the algorithm is specifically designed to match vehicles between these disruptions, as described below.

For each downstream measurement, the algorithm applies the resolution test illustrated in Figure 2-3 over the *set of feasible upstream measurements*, as defined above. The possible matches are stored in matrix format. Figure 2-4, for example, shows the possible matches for 100 vehicles measured at the downstream detector; these data were taken from the aforementioned sample of nearly 1,500 vehicles with corresponding video ground truth. The dots indicate possible matches and each row in Figure 2-4 represents the outcome from one resolution test. Note that the columns

are indexed by the difference between the arrival numbers assigned to vehicles at the upstream and downstream detector stations. It is clear that numerous possible matches resulted from each resolution test since each vehicle can only have, at most, one true match.

The algorithm then proceeds through this matrix with the ultimate goal of selecting a set of final matches. If the algorithm is successful, the final matches will correspond to the true and correct matches for the downstream vehicles. In selecting the final match from the often large collection of possible matches, the algorithm exploits the fact that consecutive vehicles will often maintain their relative order within a platoon for long distances, (Windover, 1998). As such, the true but unknown matches will often reveal themselves as relatively long sequences of possible matches that appear in neighboring rows along the same column. To this end, the algorithm proceeds through the matrix and identifies all sequences of two or more possible matches, as exemplified in Figure 2-5.

### 2.3.3 Empirical Evidence

We briefly consider all 1,500 vehicles in the sample to provide empirical motivation for the preceding steps. Calculating the number of possible matches divided by the number of pair-wise comparisons for each row, Figure 2-6A shows the cumulative distribution of the percentage of possible matches for all 1,500 vehicles. From this figure, it is clear, for example, that the frequency of false positives is less than 50 percent for seven out of 10 vehicles in this set. Because the algorithm looks for sequences, even the vehicles with a high frequency of false positives in Figure 2-6A are informative since the unlikely elements (i.e., the non-positive results) can break false sequences.

Next, using the true matches from the concurrent video, the solid line in Figure 2-6B shows the distribution of sequence lengths as measured by the algorithm for the true matches and the dashed line shows the distribution for all of the other possible matches, i.e., the false positives. The true sequences are, on average, over seven vehicles long, while the false sequences are, on average, about two vehicles long. The few long sequences of false positives are typically due to vehicles with common lengths and these sequences usually occur when there is a longer sequence of true matches.

### 2.3.4 Lane Changes and Disruptions

As previously noted, the algorithm is specifically designed to match vehicles between disruptions caused by lane changes and missed vehicle detections. After finding sequences of possible matches, the algorithm then searches for commonplace disruptions between the sequences to

continue matching in the presence of these disturbances. Figures 2-7A-C show the specific disturbances searched for. Figure 2-7A illustrates the effects of a single vehicle exiting the lane between the two stations or not being detected at the downstream station. This vehicle would have been observed downstream between vehicles m-1 and m. In Figure 2-7B, a single vehicle, m-1, enters the lane between the two stations or is not detected at the upstream station. Finally, in Figure 2-7C, either one vehicle enters and another exits the lane between stations or the vehicle length is measured incorrectly at one of the stations for the pair-wise comparison in the center of the matrix.

For each new sequence of possible matches, the algorithm checks to see if it can be linked to an earlier sequence (i.e., a sequence starting with a lower vehicle number) via one of these disturbances. The procedure is demonstrated using the sequence starting with element (m,n) in Figure 2-7D. The algorithm checks to see if there are any earlier sequences passing through one of the three shaded elements, where each element corresponds to one of the disturbances in Figures 2-7A-C. When a possible disturbance occurs, the algorithm joins the two sequences in a *modified sequence*. A *modified sequence* contains at most two distinct sequences and the definition is necessary because the subject sequence starting at (m,n) may be joined to a later sequence without regard for the possible disturbances considered here. When the algorithm creates a *modified sequence*, it simultaneously subtracts one vehicle from the total number of possible matches in the *modified sequence*; as described shortly, this penalty influences how the algorithm selects the final matches.

By following the above logic, situations will arise whereby a particular sequence might be joined with more than one earlier sequence. In Figure 2-7E, for example, there are two possible disturbances that may have preceded the first possible match in the sequence starting at (m,n). In this hypothetical instance, the algorithm joins the two adjacent sequences in the manner shown in Figure 2-7F, since this union yields a *modified sequence* with the largest number of possible matches. Note that this union does not include the last two possible matches from the earlier sequence. The exact choice of when the disturbance occurred is based on convenience, since in this case, it is impossible to determine from the matrix whether the disturbance occurred as shown or after either of the two excluded matches.

At this juncture, a given possible match will be included in a sequence and it may be included in many *modified sequences*. The algorithm will select the longest *modified sequence* (or sequence) from this set and store the sequence's length in a new matrix with the indices corresponding to the pair-wise comparison. The algorithm uses the elements in this new matrix to eliminate many of the possible matches previously defined as false positives. For each row, the algorithm retains the

element corresponding to the maximum value and discards all other possible matches in the row. The longest sequence containing the given downstream vehicle is thus retained. If more than one element contains the maximum, then the algorithm will discard all of the possible matches for that row. The remaining possible matches will henceforth be referred to as matches. Continuing the example from Figure 2-5, after applying the preceding steps to the 100 vehicles, the resulting matches are shown in Figure 2-8. Note how most matches fall near the same column in this plot. Those matches far from column 80 in this plot are likely false positives that still remain. Extending to the entire set of 1,500 vehicles with ground truth, the algorithm found a match for about 90 percent of the vehicles, which includes false positives that have not been eliminated yet. The corresponding travel times for the matches are shown in Figure 2-9. Clearly, some of the matches are due to false positives simply because the very large discontinuities between successive travel time measurements are not feasible.

### 2.3.5 Cleanup

To eliminate additional false positives, the algorithm follows three steps to "cleanup" the matches, as follows. The first step addresses the fact that a vehicle measured at the upstream station might be matched to multiple vehicles measured at the downstream station. As shown in Figure 2-10, the matches for an upstream vehicle fall on a diagonal at 45 degrees in the chosen coordinate system. It may take several minutes to observe all of the matches for a given upstream vehicle. Rather than waiting to observe the outcomes from all of the resolution tests, the algorithm uses as much information as possible immediately after identifying a match for a downstream vehicle. For the match at (m,n) in Figure 2-10, the match is discarded if its sequence length is less than that of an earlier match for the same upstream vehicle. Since the algorithm runs in real time, it can not consider the outcomes from subsequent downstream vehicles. So the upstream vehicle may still be matched to multiple downstream vehicles, but the later matches (with respect to downstream vehicle number) are stronger than any earlier ones.

Next, if several successive downstream vehicle measurements have a high frequency of false positives from the resolution test, there is a chance that the algorithm will select an incorrect sequence for these vehicles. In other words, the matrix previously shown in Figure 2-4 may not be very informative during these periods. The second step of the cleanup process recognizes that when the algorithm will select an incorrect sequence, its location will be uniformly distributed across the columns. Now recall the fact that for a given downstream vehicle the most recent upstream vehicle bounds the *set of feasible upstream matches* on the right hand side of the row. Several vehicles (and potentially a false positive associated with one of these vehicles) can usually be eliminated from the right hand side of this set simply because they would have to travel at

excessive speeds to be a true match. For the current implementation, the algorithm discards any match that would require a link velocity in excess of 85 mph.

In the third step, the assumption that lane change maneuvers and missed vehicle detections are relatively infrequent is maintained. As such, a sequence of true but unknown matches in one column is presumed to be preceded by other sequences of true matches in nearby columns. To this end, the algorithm identifies *consecutive sequences* of matches, each consisting of all consecutive downstream vehicles whose matches have the same upstream offset. This calculation is necessary because the first two steps in the cleanup will likely disrupt the earlier sequences. The algorithm then compares the upstream offset of a given *consecutive sequence* against that of the preceding eight *consecutive sequences*. If at least three of these comparisons are within ±5 columns and the current *consecutive sequence* is more than one vehicle long, the matches in the *consecutive sequence* are retained as final matches. In any event, the *consecutive sequence* is kept for later comparisons at this step.

### 2.3.6 Results

After applying the cleanup steps to the entire set of 1,500 vehicles, approximately 25 percent of the matches were eliminated. Table 2-1 shows the number of matches retained after each step while the X's in Figure 2-11A indicate the travel times from the final matches. Superimposing the travel times from the ground truth matches, it is clear that the algorithm performed quite well. The algorithm followed the increasing and decreasing travel times as disturbances passed through the link, while the local velocity measured at the detector stations ranged between 0 and 40 mph. The algorithm matched approximately 65 percent of the vehicles that passed the upstream site. One false platoon of 12 vehicles and four false positives[3] remained, yielding an error rate of 1.6 percent for this example. It is important to note that the algorithm recovered after making these errors. Finally, the time between successive matches was typically on the order of a few seconds, as shown in Figure 2-11B, with 1.3 minutes being the longest period without a reidentification.

## *2.4 A Larger Example*

No effort was made in this algorithm to match vehicles that changed lane changes. One could treat each lane as an independent process and integrate the results from all lanes for a more robust indicator. An obvious extension to this work would be to look across all upstream lanes rather

[3] These false positives fell at the start or end of sequences consisting mostly of true matches.

than a single lane. Nonetheless, as demonstrated in this Section, the algorithm works using data from a single lane.

Figure 2-12 shows an example of vehicle reidentification over a much larger set. In this case, the algorithm was applied to all five lanes over an 1,800 foot segment of westbound Interstate 80 in Berkeley, California. The resulting travel times for matched vehicles are shown with dark points and the three hours shown in the figure include the onset of the morning peak. The algorithm matched between 40 and 55 percent of the passing vehicles in each lane during this period, even though the sample includes many free flow vehicles. Between 7:00 and 9:00, the most congested period, the algorithm found a match for 61 percent of the vehicles. Following Caltrans convention, the lanes are numbered from the inside out, and lane one is a high occupancy vehicle (HOV) lane.

The process of manually generating ground truth data would be prohibitively labor intensive for the 25,000 vehicles in this sample. Coifman (2001) presents a methodology to estimate link travel times using data from a single detector station. Applying the estimation technique using data from the upstream detector, and then repeating the estimation using data from the downstream detector, yields the two lines in each of the plots. Except for a few transient errors, the pair of estimates bound the measured travel times in each of the lanes as disturbances propagate through the link. Unlike the measurement algorithms presented in this document, the estimation technique can not capture changes in travel time due to delay causing events within the link. Using the two procedures in conjunction, significant deviations between the two methods should be indicative of an incident or a recurring bottleneck within the link.

## *2.5 Conclusions*

This Section has presented a new algorithm to match a vehicle's length measurement at a downstream detector station with that vehicle's corresponding measurement at an upstream station. The algorithm rules out unlikely matches, looks for sequences of possible matches between measurements at the two stations and then eliminates unlikely sequences of these matches.

The beauty of the approach is in its simplicity. Matching vehicles between detector stations is a difficult task. Preceding research efforts emphasized computationally intensive and/or hardware intensive strategies. By creating the solution space of possible matches, the algorithm facilitates vehicle reidentification using existing detector hardware and inexpensive computers. It is left to future research to determine the optimal parameters for the algorithm, as well as the relationship between station spacing and algorithm performance. To this end, work is underway to develop the

Berkeley Highway Laboratory (BHL), which includes eight dual-loop-detector stations and machine vision vehicle tracking tools to ease the ground truth data collection (Section 4). The BHL already uses the algorithm presented above to measure travel time in real time.[4]

The contribution of this work to the field of traffic surveillance should prove to be significant since the vehicle reidentification algorithm will allow the study of travel time applications without deploying new hardware and thereby enable cost-benefit analysis before investing in a new detection system. If travel time measurement proves to be beneficial, the algorithm could be deployed using dual-loop-detectors, or it could be transferred to new detector technologies that have better measurement accuracy. It is worth noting that the additional hardware cost per station to deploy the algorithm across all lanes in the BHL is less than one percent of the cost to install a detector station for conventional traffic surveillance. The methodology should prove beneficial for research purposes as well; yielding better insight into vehicle dynamics between widely spaced detector stations without the host of assumptions necessary with simulation.

Finally, it is worth discussing the percentage of passing vehicles that must be matched for surveillance. For example, Origin/Destination studies would likely require near perfect performance from non-AVI vehicle reidentification systems. But travel time measurement is not as demanding, Van Aerde et al. (1993) estimated that matching 20 percent of the population is sufficient for such measurements while Holdener and Turner (1996) suggest that the percentage may even be smaller. Using dual-loop-detector data, the algorithm has already surpassed these guidelines for travel time measurement.

[4] The real time system can be viewed at: http://www.its.berkeley.edu/projects/freewaydata.

Figure 2-1, The segment of Interstate-80 in Berkeley, California used for this study.

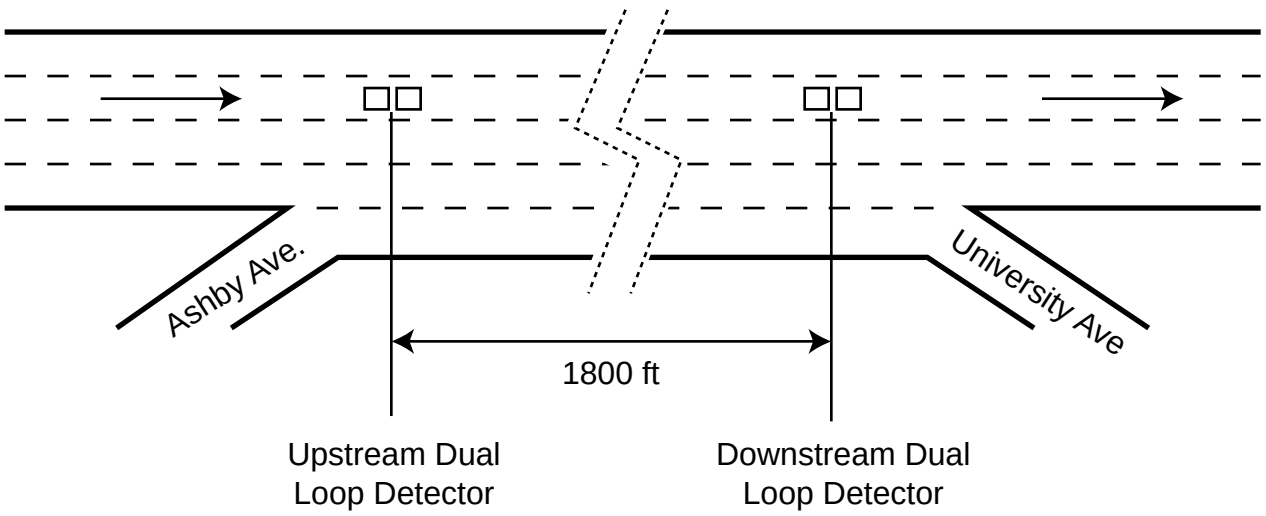

Figure 2-2, One vehicle passing over a dual-loop-detector, (A) the two detection zones and the vehicle trajectory as shown in the time space plane. The height of the vehicle's trajectory reflects the non-zero vehicle length. (B) The associated turn-on and turn-off transitions at each detector.

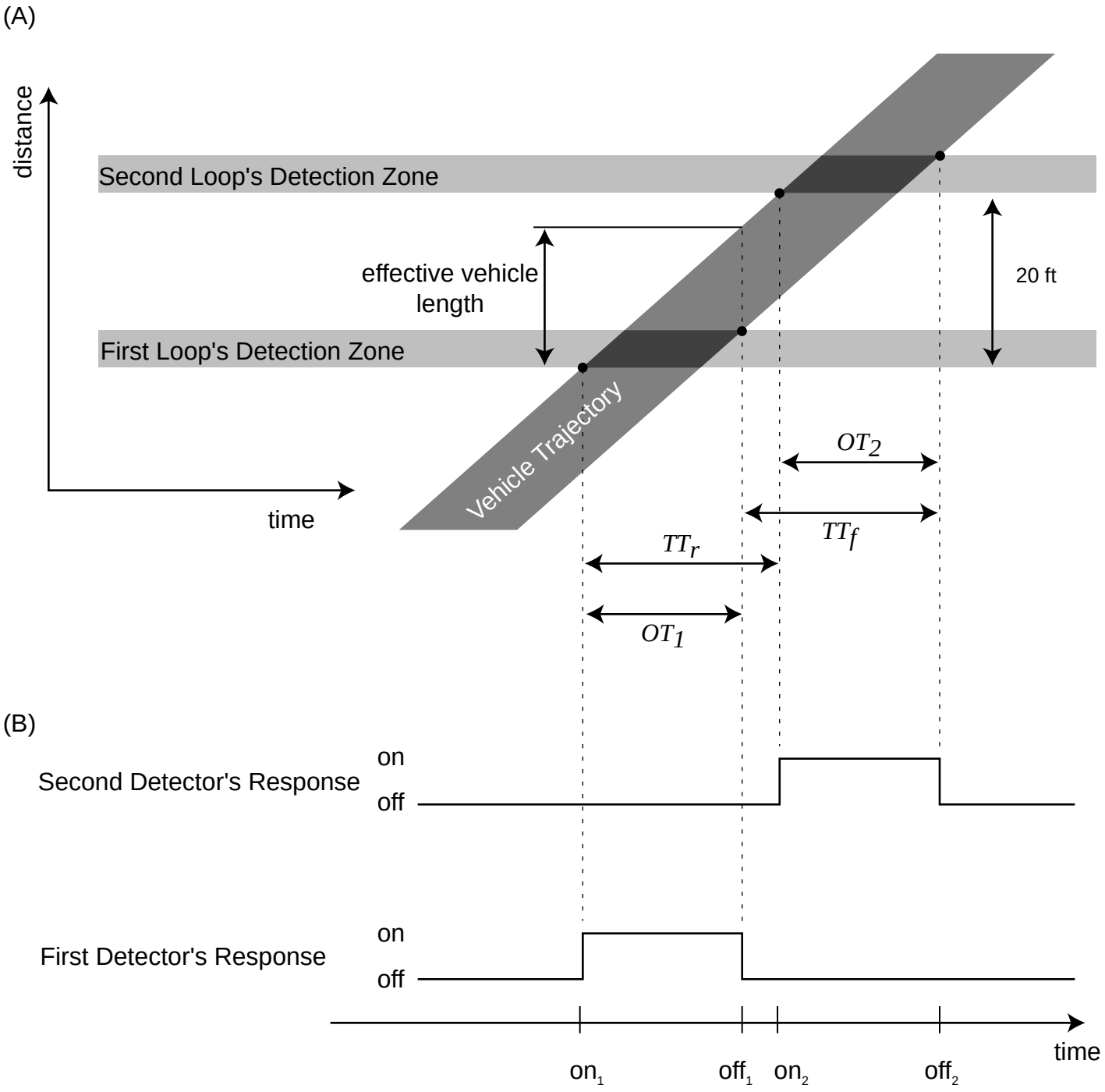

Figure 2-3, (A) "Resolution test" between one downstream vehicle and a set of upstream vehicles. If the upstream measurement range does not intersect the downstream measurement range, the upstream vehicle can be dismissed as being an unlikely match for the downstream vehicle. (B) Everything that can not be eliminated are considered possible matches, as indicated with open circles. Note that each outcome is shown directly below the given comparison from part (A).

(A)

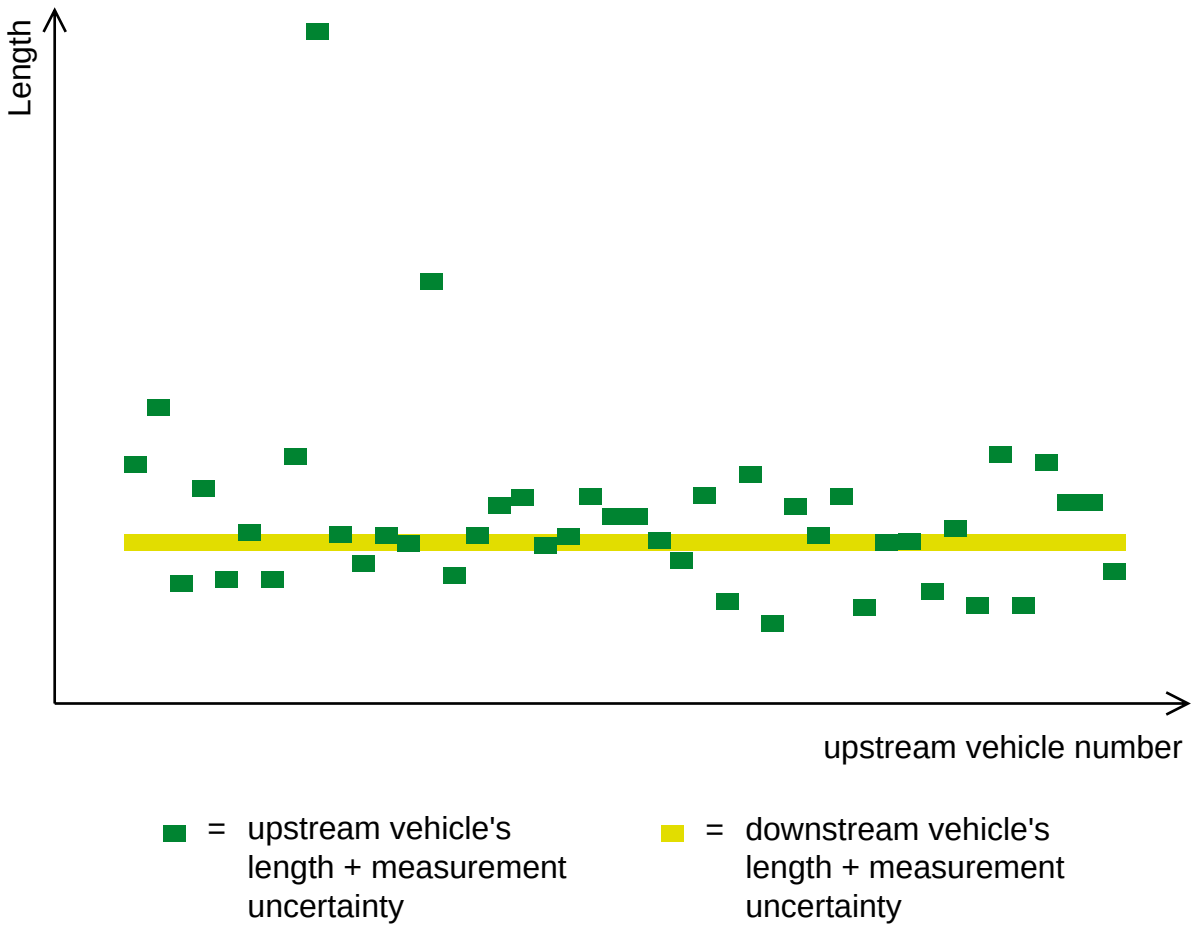


(B)

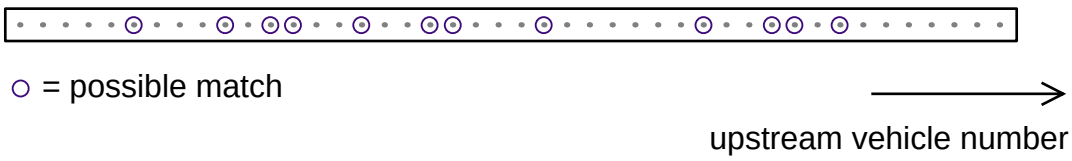

Figure 2-4, Consider a set of 100 downstream vehicles, applying the resolution test to each of these vehicles produces a set of possible matches, or one row in this matrix. Note that the columns are indexed by the upstream offset, so, if there were no lane changes in this coordinate system, all of the true matches would fall into a single column.

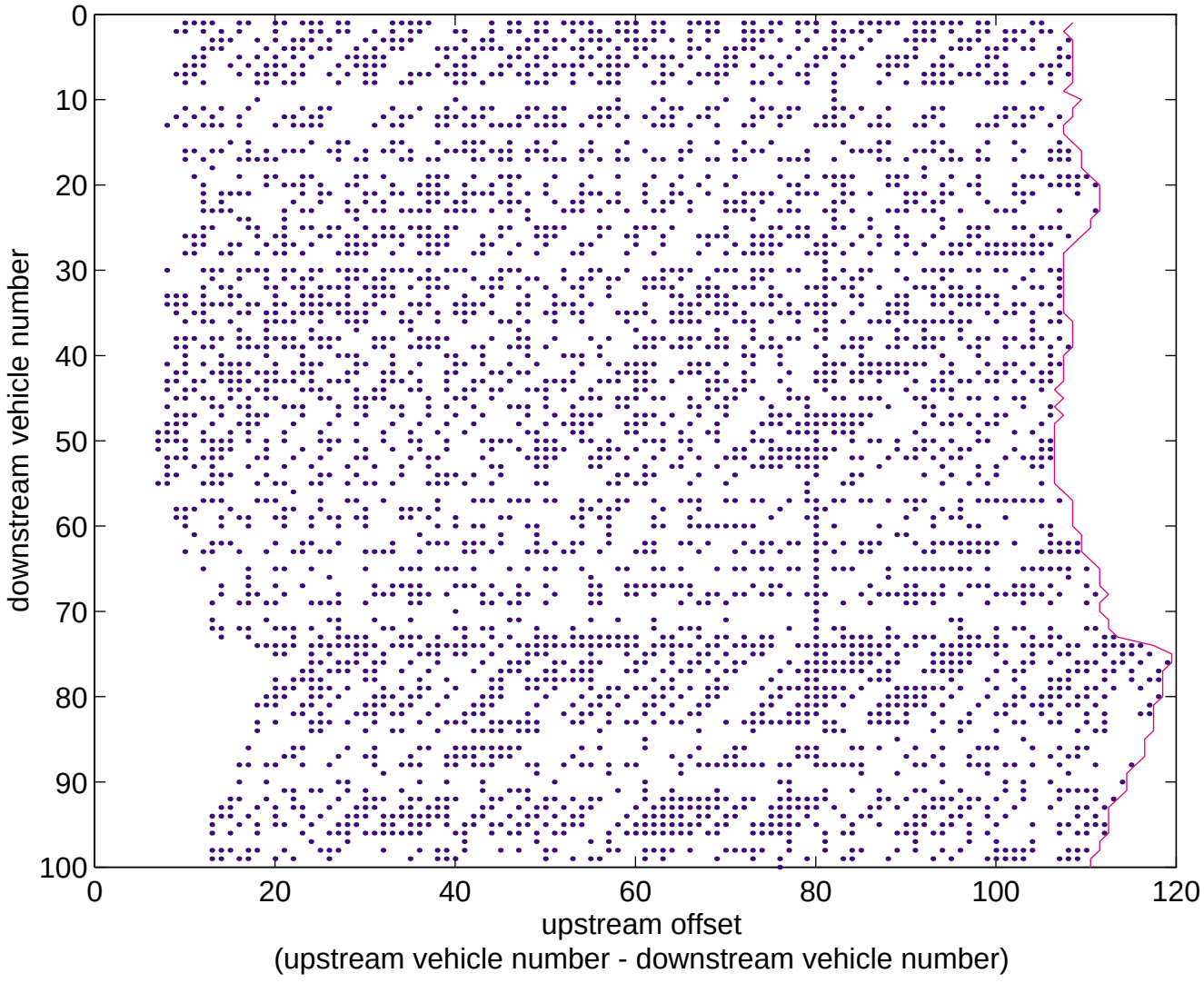


= boundary line indicating the last feasible match for each downstream vehicle

= possible match

Figure 2-5, All sequences of two or more possible matches for the on-going example.

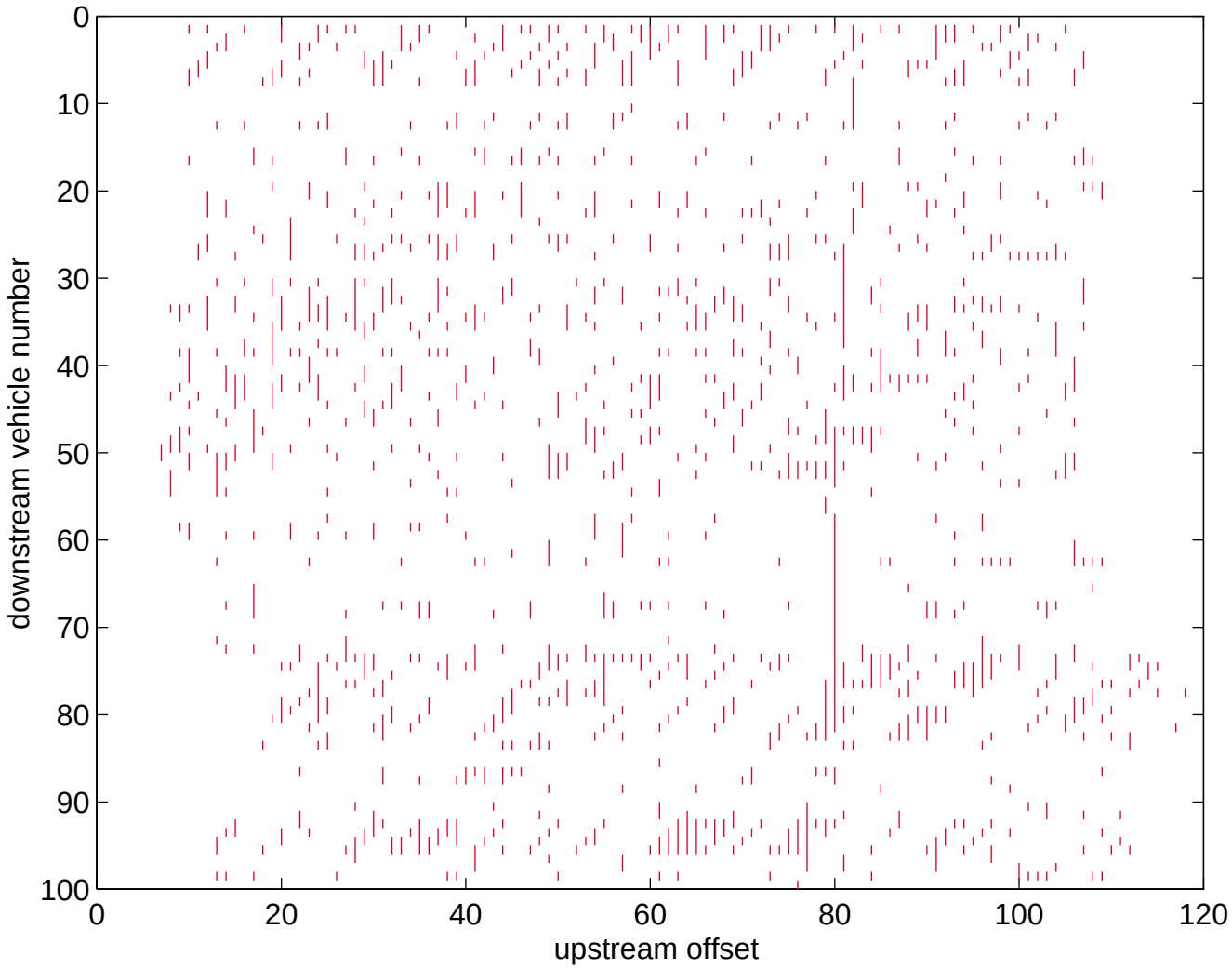

Figure 2-6, (A) The cumulative distribution of the percentage of possible matches for all 1495 downstream vehicles. (B) Using concurrent video to calculate the true matches, the solid line shows the cumulative distribution of sequence lengths measured by the algorithm for these matches. While the dashed line shows the cumulative distribution of sequence lengths for all other possible matches, i.e., the false positives.

(A)

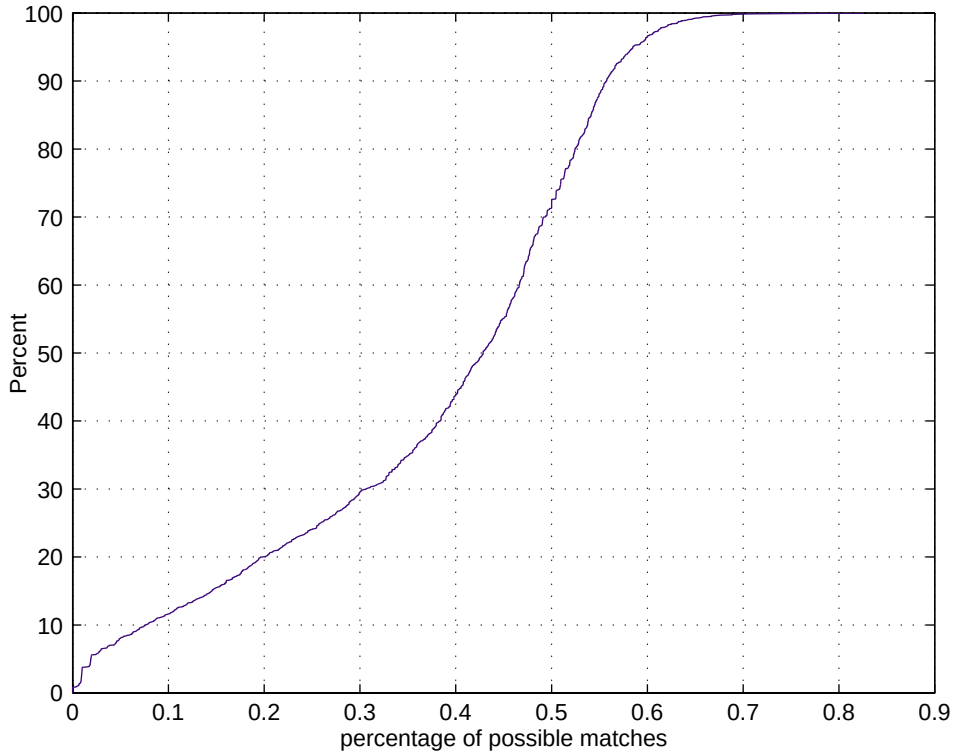


(B)

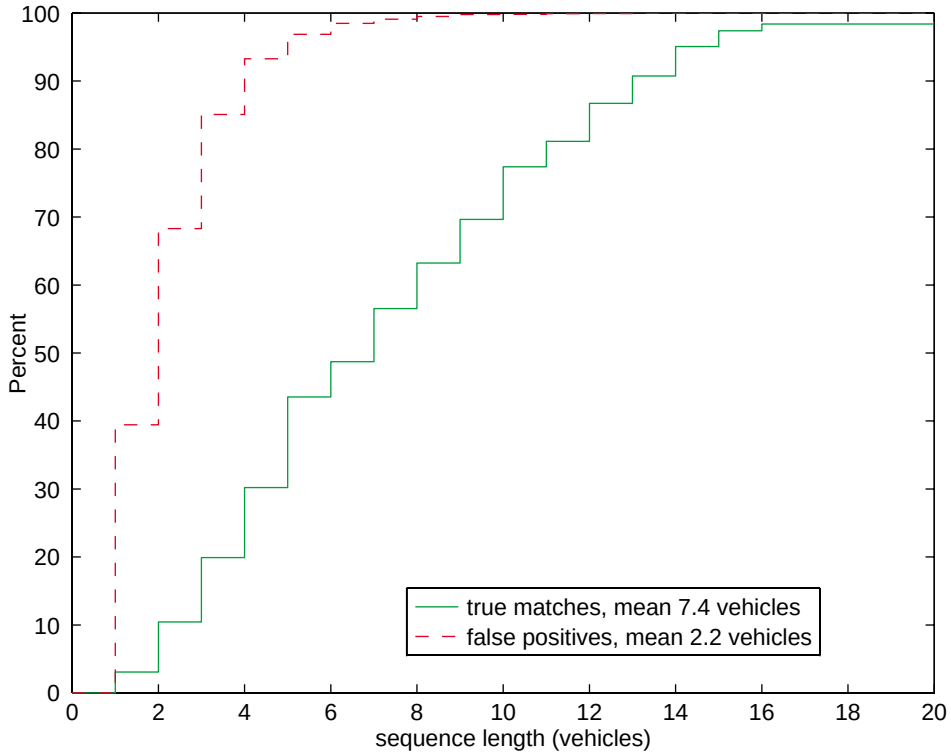

Figure 2-7, A simple example illustrating the possible disruptions recognized by the Algorithm: (A) One vehicle exits the lane between stations or is not detected downstream, (B) One vehicle enters the lane between stations or is not detected upstream, (C) One vehicle enters and one vehicle exits the lane between stations or is measured incorrectly at one of the stations, (D) The search region for the sequence starting at element (m,n). (E) Three sample sequences, one in each column n-1 to n+1. (F) In this case, the sequence starting at (m,n) is joined via an entrance (part (B)) to a portion of an earlier sequence.

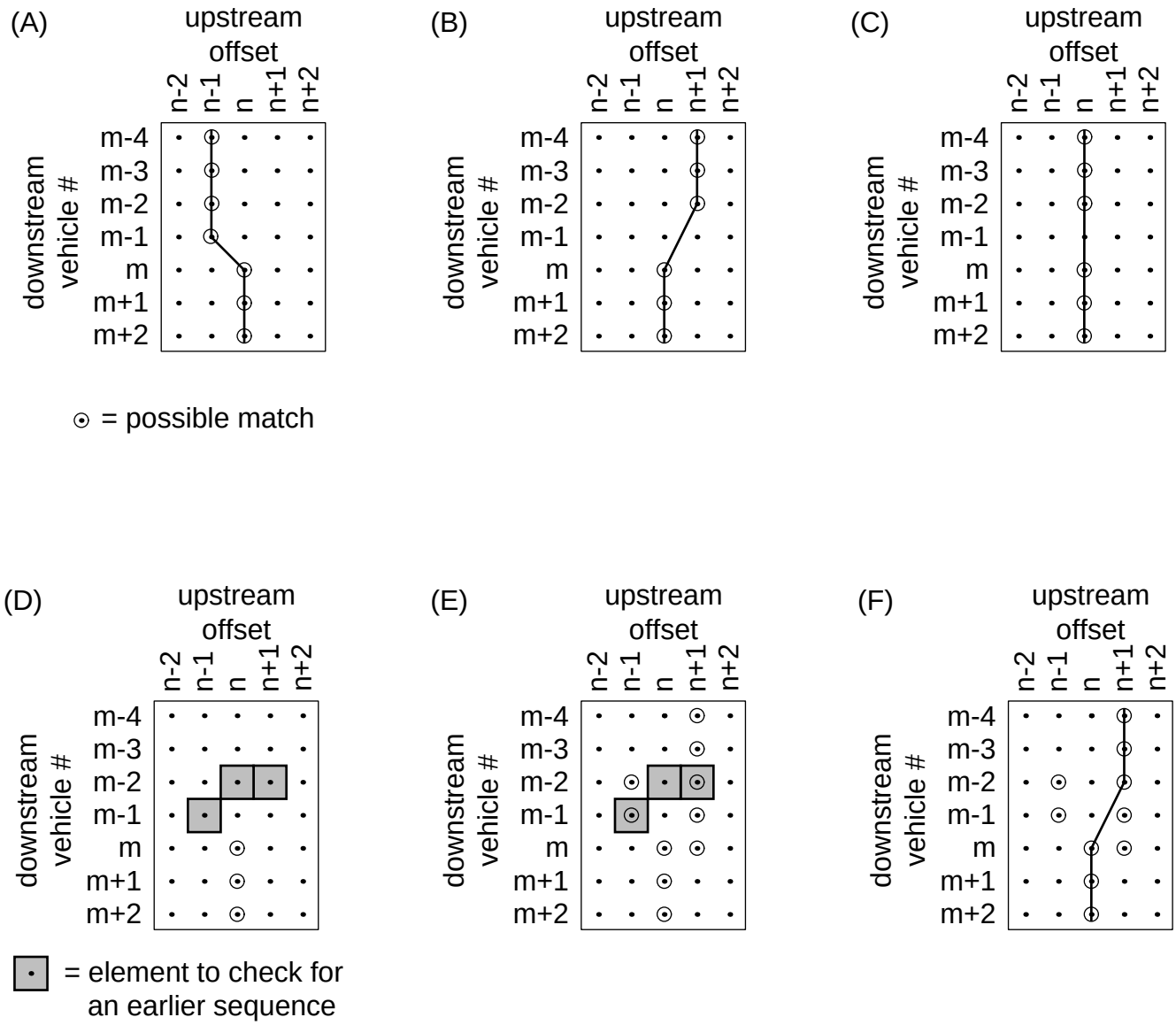

Figure 2-8, The resulting matches for the on-going example after allowing for lane changes. Each match corresponds to the longest modified sequence for the given downstream vehicle. Note how most matches fall near column 80 with small column shifts due to lane change maneuvers.

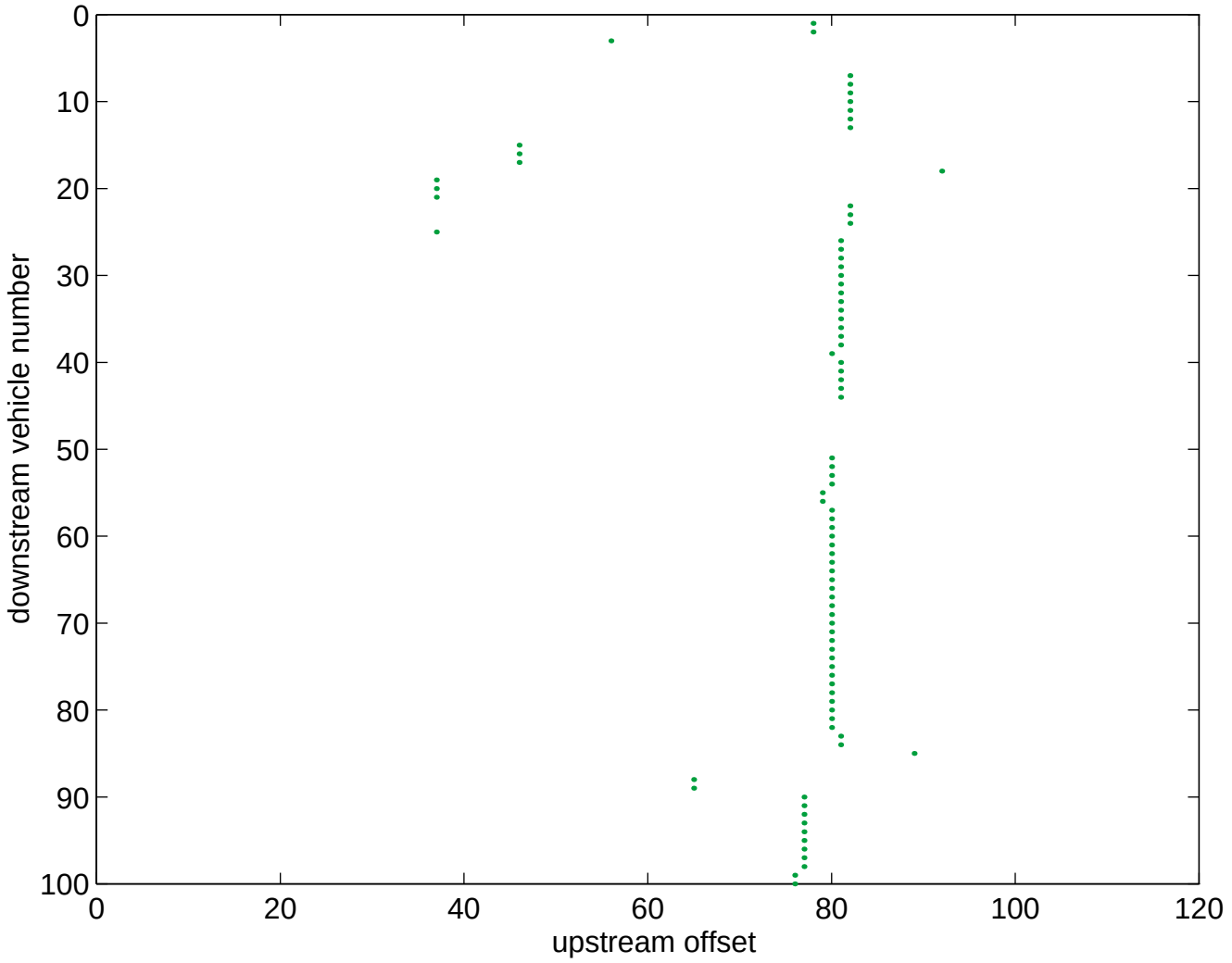

Figure 2-9, After applying the algorithm to 1495 vehicles, 1345 vehicles were matched by the algorithm. This figure shows the resulting travel times for the matches. Most of the travel times seem plausible; but clearly, there are a significant number of erroneous matches, manifest as random noise.

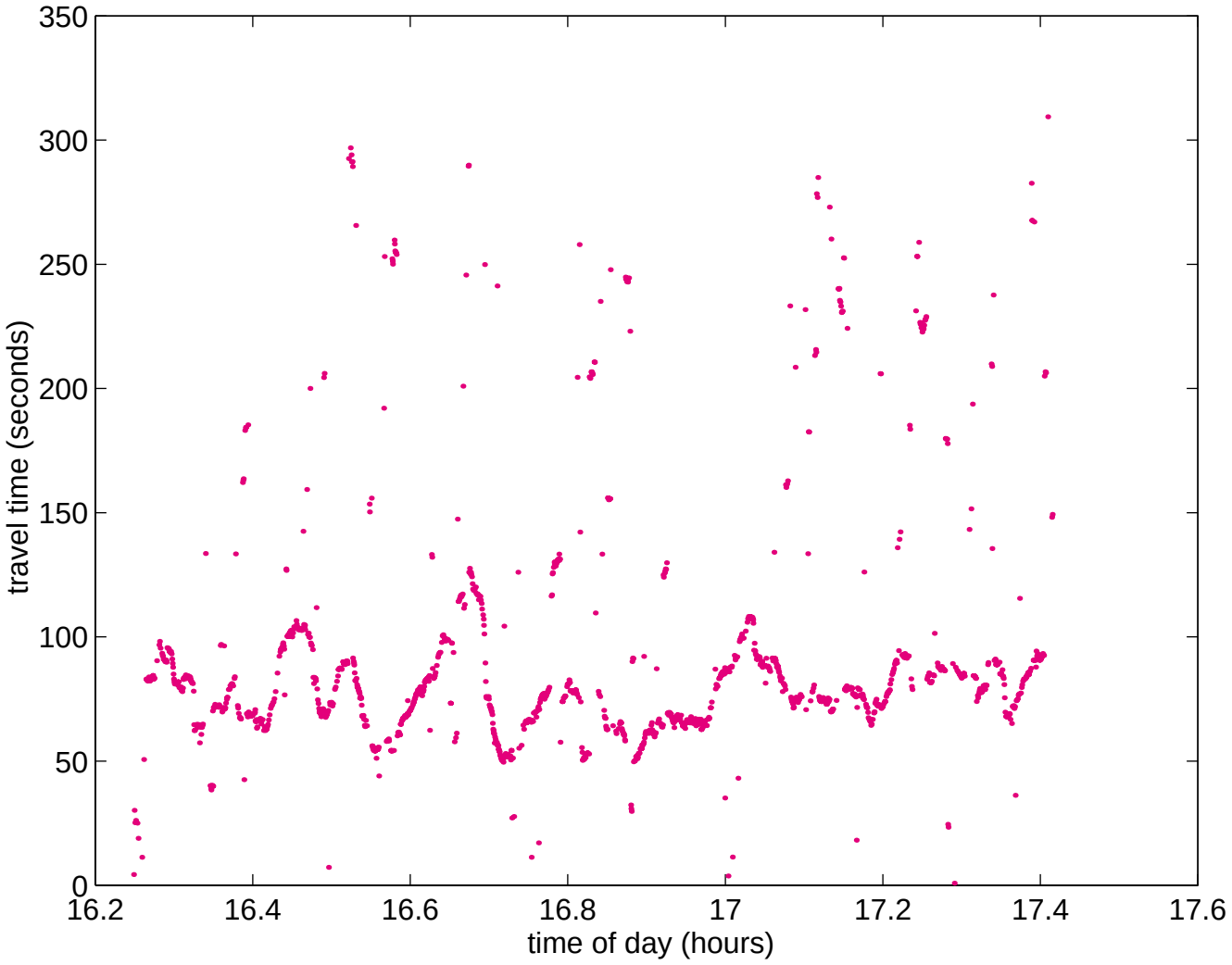

Figure 2-10,Each match is compared to any earlier matches for the upstream vehicle (i.e., the diagonal line for the match at (m,n)). The match is discarded if its sequence length is less than that of an earlier match for the same upstream vehicle. The comparison does not consider matches from later downstream vehicles since the algorithm runs in real time.

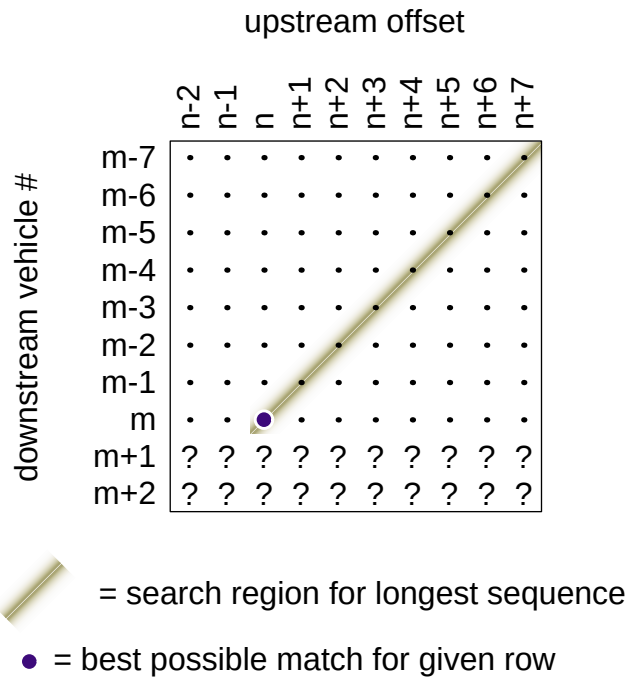

Figure 2-11, (A) Compare the travel times for the 1008 final matches against those from the ground truth matches. (B) The time between successive final matches.

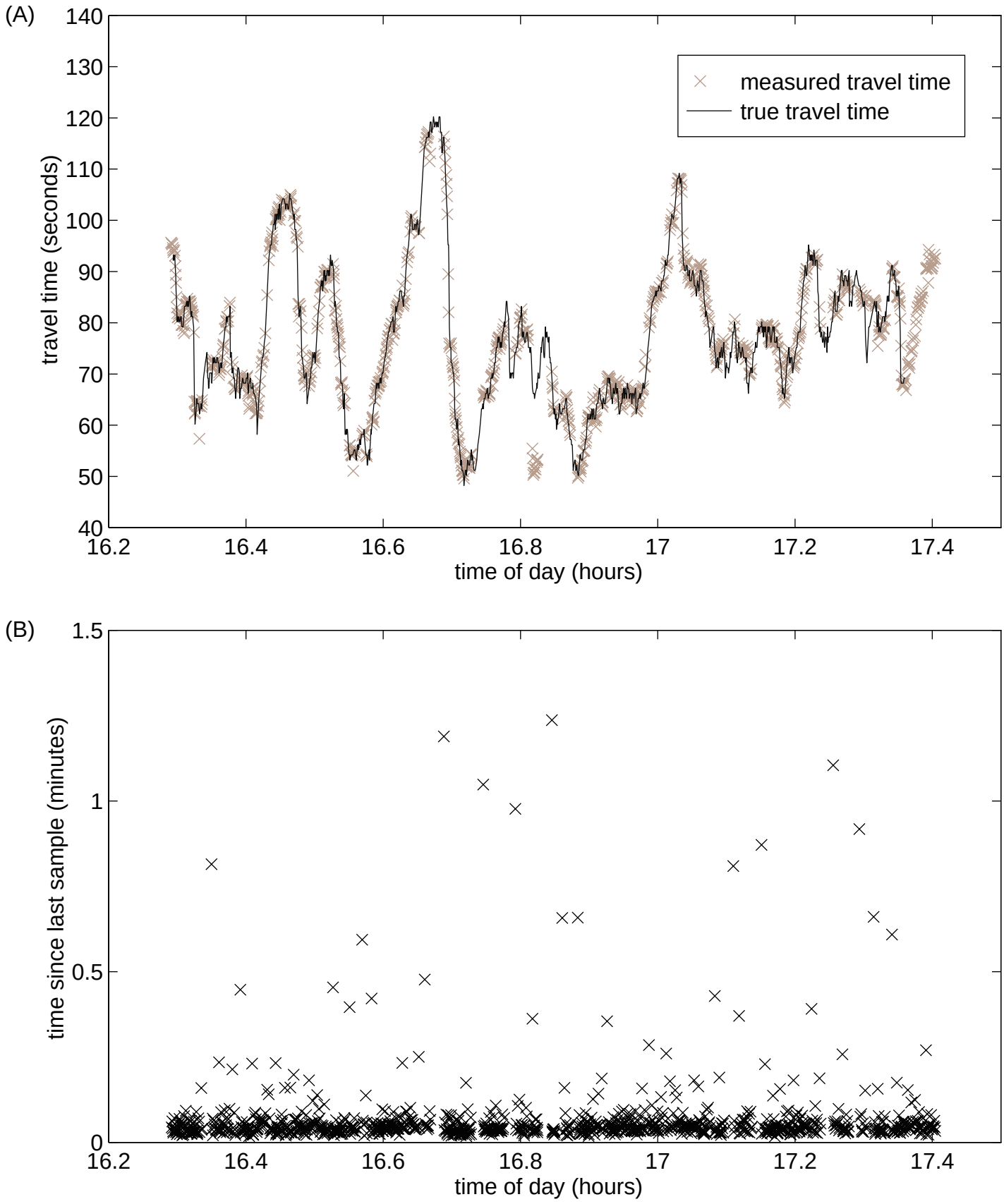

Figure 2-12, A comparison between measured travel times and estimated travel times for three hours, across five lanes, over an 1,800 ft segment.

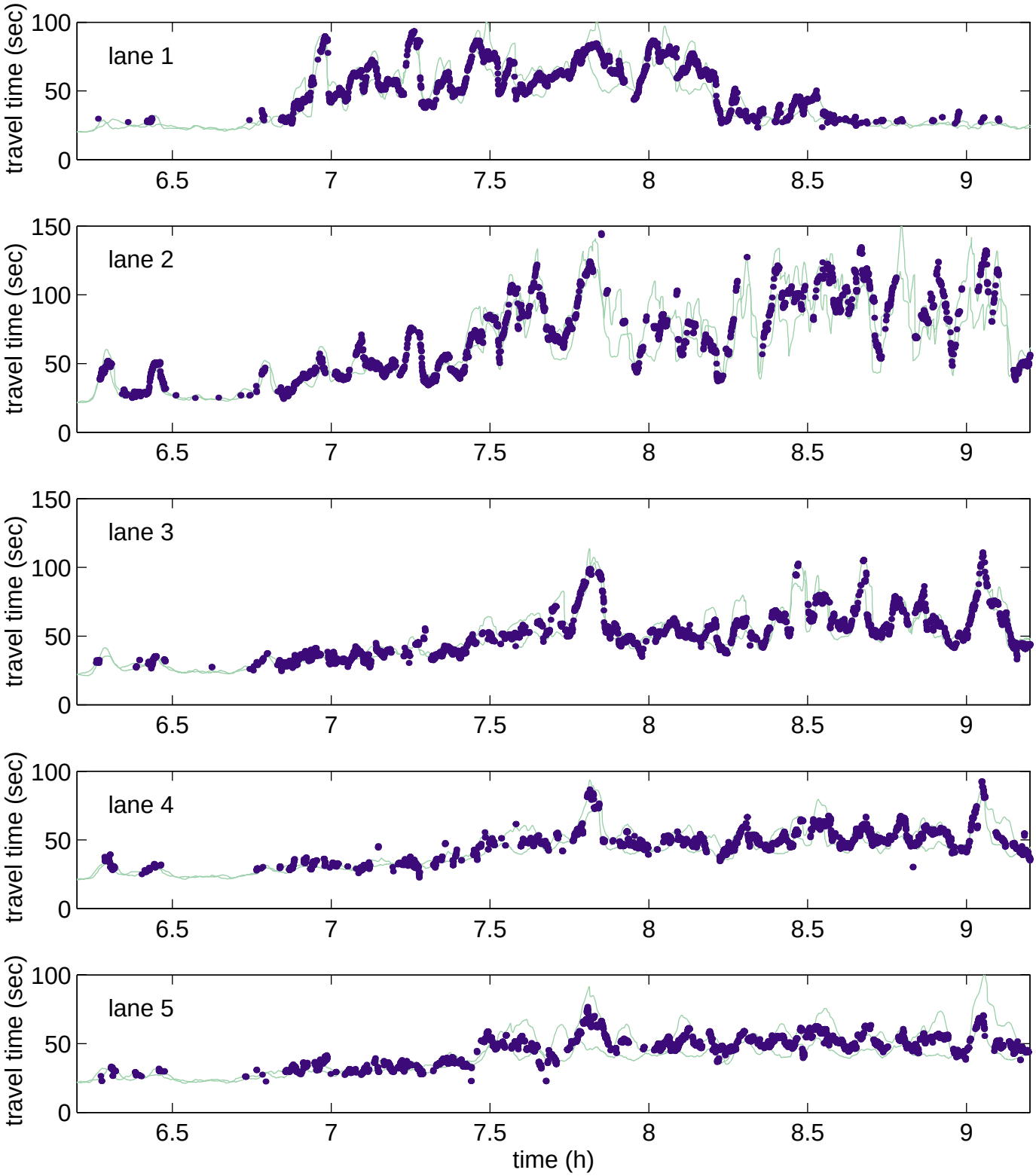

Table 2-1, Number of matches after each cleanup step for the on-going example.

| Step | Number of Matches |
|---|---|
| pre-cleanup | 1345 |
| step 1 | 1212 |
| step 2 | 1202 |
| step 3, final matches | 1008 |

# 3 VEHICLE REIDENTIFICATION AND TRAVEL TIME MEASUREMENT, PART II: UNCONGESTED FREEWAYS AND THE ONSET OF CONGESTION

## *3.1 Introduction*

Traditional traffic surveillance strategies use loop detectors to calculate aggregate measures, such as flow and occupancy, at discrete locations on a freeway. Typically, these point measurements are assumed to be representative of extended links spanning detectors. This assumption is usually not valid when the facility becomes congested, e.g., when an incident occurs between two detector stations it can take several minutes before measured speeds drop at either of the stations.

The limitation of point data has spurred interest in vehicle reidentification techniques, which match the observations of the same vehicle at successive detector stations (e.g., Reijmers, 1979, Pfannerstill, 1984, Kühne and Immes, 1993, Huang and Russell, 1997, Cui and Huang, 1997). All of these earlier works require new detector hardware to extract detailed vehicle *signatures*. Often times, these advanced technologies are developed without consideration for the general goals of traffic surveillance, and as a result, an operating agency may risk investing in an expensive surveillance system to capture extraneous information. The systems also risk discarding useful information, e.g., in some cases, the tools collect link data but are not capable of measuring point data.

From an operations standpoint, the most important task of a surveillance system is determining reliably whether the facility is free flowing or congested. The second most important task is responding rapidly when the facility becomes congested. Other tasks, such as quantifying the magnitude of congestion, are desirable, but tertiary. Conventional loop detector surveillance satisfies the first and tertiary tasks, but the response time to delays between detector stations can be excessive (Lin and Daganzo, 1997). Some of the advanced surveillance technologies promise to satisfy all of these tasks, but they have yet to see widespread deployment. In contrast to investing in new detector hardware before evaluating the benefits of vehicle reidentification, this Section proposes an interim surveillance algorithm using existing dual loop detectors in a new way. The approach will improve the performance of these detectors on the first and second tasks. It will also provide a means for operating agencies to assess the need for the more accurate systems that require new hardware, prior to making a substantial investment.

The algorithm identifies relatively distinct vehicles[5] at the downstream detector station and then for each of these vehicles, it looks for a similar vehicle in the same lane at the upstream station within a time window of *reasonable* free flow travel times. Thus, if traffic is free flowing over the link between detectors, this approach will usually find a match in the time window. If the freeway is congested, vehicles will be delayed and the true match for a vehicle will not be found in the time window. In the event a match is found, the algorithm can also address the tertiary tasks, such as calculating that vehicle's travel time. In other words, the algorithm is capable of reporting free flow travel times or the fact that "traffic is not free flowing". In the latter case, a complementary reidentification method can be used to measure travel time during congestion, as presented in Section 2, if the metric proves to be desirable.

To illustrate the potential benefits of the new system, consider incident detection using point detectors. Lin and Daganzo (1997) note that two signals emanate from an incident, a backward moving shock wave and a forward moving drop in flow. Without link travel time information, detection of an incident can happen only when both of these signals have been received at the detector stations. Although the drop in flow travels at the prevailing traffic velocity, Lin and Daganzo estimated the shock wave velocity to be on the order of 13 km/h. Fortunately, the drop in flow reflects the fact that vehicles are being delayed behind the incident. So rather than waiting for the slow moving shock wave, the new algorithm could be used to quickly identify the onset of delay corresponding to the drop in flow.

### *3.2 Is Traffic Free Flowing?*

All vehicles that traverse a link between two detector stations must, by definition, pass both stations. For these vehicles, every downstream observation should have a corresponding upstream observation and the time between these two observations is simply that vehicle's link travel time. These travel times are not known a-priori; however, if the vehicle travels at free flow velocities over the entire link, the travel time must fall within a known range of free flow travel times. This concept is illustrated in Figure 3-1. For the present study, the free flow travel time range is defined as follows:

$$ttR_0 = \left[ \frac{\text{distance}}{\max(v+16,88)}, \quad \frac{\text{distance}}{\max(v-16,72)} \right] \tag{3-1}$$

[5] Because vehicle length can be measured at dual loop detectors, long vehicles satisfy this criterion. The reader should note, however, that the algorithm would be equally applicable to any other identifiable vehicle feature, perhaps as measured with a different type of vehicle detector.

where

$ttR_0$ = the range of feasible free flow travel times [hours],
$v$ = local velocity measurement at the downstream detector station [km/h],
distance = the known distance between detector stations [km].

To keep the search window as short as possible, while also being able to accept a wide range of free flow velocities, Equation 3-1 will select the assumed velocity range to be [72,88] km/h if v<72 km/h and v±16 km/h if v>88 km/h.[6]

Chang and Kao (1991) suggest that at most locations, lane change maneuvers are relatively infrequent during free flow conditions.[7] So a free flow vehicle observed at the downstream station will usually have a corresponding observation at the upstream station in the same lane, in the time window bound by $ttR_0$. Congestion will disrupt this relationship, both because the travel time will increase beyond the free flow travel time range and because there may be an increase in lane change maneuvers, particularly if one or more lanes are blocked.

### 3.2.1 Parameter Measurement

For a given downstream vehicle, many upstream vehicles may be observed in the corresponding time range. As discussed in Subsection 2.3, effective vehicle length is used to differentiate between vehicles. Under free flow conditions, the two traversal times shown in Figure 2-2 should be approximately equal because any acceleration is negligible during the short period that a vehicle is over the detector; similarly, the two on-times should be approximately equal. For this Section, each pair of measurements is reduced to a single value using the harmonic mean,

$$TT = \frac{2}{1/TT_r + 1/TT_f} \tag{3-2}$$

$$OT = \frac{2}{1/OT_1 + 1/OT_2}$$

Equation 3-2 is used to reduce the impact of occasional measurement errors, but the method also works using just one of the traversal times and one of the on-times for each vehicle. From Figure

[6] Note that these constants were determined empirically, but they have proven robust when applied to many different freeway links.
[7] The experimental results in subsequent subsections support this observation.

2-2A, vehicle velocity is simply the loop separation, 6.1 m for this study, divided by the traversal time. The effective vehicle length, *L*, is the velocity multiplied by the on-time,

$$L = \frac{6.1 \cdot OT}{TT} \quad [\text{m}] \tag{3-3}$$

The controller samples the loops at 60 Hz, so at best, each parameter in Equation 3-2 is accurate to 1/60 seconds. Assuming the times from Figure 2-2 are expressed in seconds, the length range, *LR*, is defined as:

$$\begin{aligned} LR &= [\text{minimum length estimate}, \quad \text{maximum length estimate}] \\ &= \left[ 6.1 \cdot \frac{OT - 1/30}{TT + 1/30}, \quad 6.1 \cdot \frac{OT + 1/30}{TT - 1/30} \right] \quad [\text{m}] \end{aligned} \tag{3-4}$$

and the measurement uncertainty is defined as the difference between the maximum and minimum length estimates. Of course the occasional measurement error, such as a vehicle changing lanes over the detector, will result in an erroneous *LR* for that vehicle; but the methodology was specifically designed to accommodate these errors. Finally, to ensure the best measurements possible, any hardware problems such as cross talk between detectors are identified using Coifman (1999) and corrected.

As previously noted, the algorithm compares observations, or length measurements, between detector stations. If the length range for a downstream observation overlaps that of an upstream observation, then the two observations may have come from the same vehicle. Otherwise, the result of the pair-wise comparison can be dismissed as an unlikely match because even allowing for the measurement uncertainty, the two ranges do not intersect.

Unfortunately, most observations fall in a small range, which is on the order of the measurement uncertainty during free flow conditions. For example, Figure 3-2 shows the distribution of observed vehicle lengths over 24 hours at one detector station. Roughly 80 percent of the observations fall between 5 m and 7 m. During free flow conditions, the measurement uncertainty is on the order of 0.7 m for these short vehicles, making difficult the task of differentiating between them. In contrast, some length observations are as long as 24 m. The large range of feasible lengths and the lower frequency of observations for the long vehicles make it possible to differentiate between them even at free flow velocities.

### *3.3 Algorithm Implementation*

Using an example to illustrate the algorithm implementation, consider the 2.1 km freeway segment from the BHL shown in Figure 3-3. To eliminate the common vehicles, all downstream vehicles shorter than 7 m are ignored. Whenever a long vehicle passes the downstream dual loop detector, the algorithm searches a fixed time earlier, bounded by Equation 3-1, for any upstream vehicles in the same lane whose length range, as defined by Equation 3-4, intersects the downstream vehicle's length range. If an intersection is found, the corresponding upstream vehicle is considered a possible match. If more than one intersection is found within the time window, then arbitrarily, the most recent of these upstream observations is considered the possible match. Otherwise, the downstream vehicle does not have an identifiable free flow match in the lane.

Obviously, a free flow vehicle will not have a match in the same lane if the vehicle changed lanes, entered the freeway between detectors, or because of a misdetection at one of the stations. On the other hand, a delayed vehicle should not have a match, but a false positive may fall within the time window. To eliminate most of these transients, the algorithm takes a moving average of the 10 most recent outcomes (including the current outcome), where a possible match is assigned a value of one and a non-match is assigned a value of zero. Figure 3-4 shows this moving average for just over 2.5 hours of data from the two dual loop detectors. Applying an arbitrary threshold to these data, Figure 3-5 shows the travel times for all of the long vehicles that had a possible match and a moving average over 0.5. These free flowing matches will be referred to as *fast matches*.

Generating ground truth data to verify the algorithm is complicated by the simple fact that vehicle reidentification over extended distances is inherently difficult, both for an automated system and for a human. It is prohibitively time consuming for a human to generate exact matches for a large number of vehicles. Fortunately, it is not necessary to match every vehicle manually. If the algorithm is correctly matching vehicles, it will also yield the true travel times for those vehicles. Although travel time over a freeway link can change dramatically in a short period of time, the travel times for two successive vehicles will be very similar. Thus, the observer must manually match a sufficient number of vehicles to capture changes in link travel time, but this can be accomplished using a small fraction of the passing vehicles. To this end, the study used video data recorded concurrently with the dual loop detector data and an observer matched all visually distinct vehicles that passed both detectors in the lane during the study period. The resulting travel times are shown with stars in Figure 3-5. Finally, Table 3-1 shows that 7.4 percent of the vehicles were long vehicles in this example and 71 percent of these vehicles were matched. At first glance, this low rate of detection may not seem very useful. But one must keep in mind that traffic is free flowing when the matches are found, so travel times are relatively constant. Furthermore, the goal

of the algorithm is to detect when travel times start to increase, which is the subject of the next Subsection.

### *3.4 Detecting the Onset of Congestion*

The onset of congestion is characterized by a dramatic increase in link travel times. When this occurs, the true travel times will not fall within the range specified by Equation 3-1. Notice that the algorithm did not find any *fast matches* after 14.7 hours, which corresponds to the time when the ground truth travel times start increasing due to a queue overrunning the downstream station. Although the measured travel times in Figure 3-5 are useful for traffic surveillance, the true diagnostic power of the method comes from the moving average in Figure 3-4. The free flow periods are characterized by high average values and congested periods by low values. Unfortunately, there is significant noise in these measurements. During free flow conditions, most of this noise is due to the presence of the two ramps and the long distance between stations. Both of these factors increase the probability that a free flow vehicle will change lanes and thus, it will not have a match in the same lane. On the other hand, the long distance between detectors increases the time range in $ttR_0$ and thus, increases the probability of finding a false positive during congested conditions.

To filter out most of the false positives, consider the number of unmatched vehicles preceding each *fast match*, as shown in Figure 3-6A. Each of the matches preceding the onset of congestion at 14.7 hours have few preceding unmatched vehicles while most of the matches after the onset have many preceding unmatched vehicles. The contrast between the two groups can be increased by taking a moving sum over this data, e.g., Figure 3-6B shows the results after taking a moving sum of two samples. To eliminate the false positives, all *fast matches* that have more than four unmatched vehicles in Figure 3-6B are discarded. Figure 3-7 shows the results after recalculating the moving average over all outcomes. Note that the process has eliminated all of the noise during congestion.

### *3.5 Extending Surveillance into Congested Conditions*

Looking closer at the ground truth travel times in Figure 3-5, there is a transition as the queue first overruns the downstream detector and eventually covers the entire link. This transition is characterized by increasing travel times. In an attempt to capture the increasing delays during the transition, four additional travel time ranges are defined:

$$ttR_1 = \left[\frac{\text{distance}}{80}, \quad \frac{\text{distance}}{64}\right]; \qquad ttR_2 = \left[\frac{\text{distance}}{72}, \quad \frac{\text{distance}}{56}\right]; \qquad (3\text{-}5)$$
$$ttR_3 = \left[\frac{\text{distance}}{64}, \quad \frac{\text{distance}}{53}\right]; \qquad ttR_4 = \left[\frac{\text{distance}}{56}, \quad \frac{\text{distance}}{45}\right]$$

where the denominators in the bracketed expressions bound the possible link velocities [km/h] for each set. Also notice how all five ranges overlap.

As the queue grows across the link, the true travel times will pass from $ttR_0$ to $ttR_1$, and so on through $ttR_4$, until finally the travel time exceeds all five ranges. Repeating the analysis presented in the previous Subsection (i.e., Figure 3-7) for $ttR_1$ and $ttR_2$ yields the dashed lines in Figure 3-8A. Notice how the curve for $ttR_1$ starts increasing before $ttR_0$ drops due to congestion, and similarly the curve for $ttR_2$ relative to $ttR_1$. This plot also shows a few false positives, such as the rise in $ttR_2$ at 14.85 hrs. Once the link becomes sufficiently congested, the history implicit in the moving average is lost and the method can not differentiate between false positives and true matches. To reduce the influence of false positives in the longer travel time ranges, the algorithm will only accept a sequence of non-zero values if the next faster *ttR* moving average is non-zero at the start of the sequence. Thereby allowing the algorithm to follow increasing travel times, but blocking any long travel times once the travel time has exceeded $ttR_4$. This process is evident in the right hand side of Figure 3-8B, where the false positives have been discarded. Finally, the algorithm selects the range with the highest average value at the given instant, as shown in Figure 3-8C. Figure 3-9 shows the resulting travel times after extending the method to $ttR_3$ and $ttR_4$. The algorithm does not find any matches once the queue has covered the entire link and the ground truth travel times level off.

### *3.6 Response Time and Algorithm Extensions*

After the onset of congestion in the preceding example, it took 3.5 minutes for the $ttR_0$ moving average to go to zero (Figure 3-7), clearly indicating that the link travel time had exceeded the time range. Combining the information from multiple time ranges yields a more responsive indicator. The moving average for $ttR_1$ exceeds the respective measurement for $ttR_0$ just 15 seconds after the last free flow vehicle was observed (Figure 3-8B), rapidly indicating that the travel time has exceeded $ttR_0$. In contrast, using the empirically measured end-of-queue velocity reported in Lin and Daganzo (1997), it would have taken approximately 9 minutes for the queue to span the entire link. Looking at the local detector data, it actually took the queue 10.5 minutes to span the link.

After the queue reaches the upstream detector, following conventional practice, it would then take several additional sample periods[8] to differentiate between a transient event and an actual drop in velocity. Of course the response time of the present algorithm is a function of truck frequency. In this case the long vehicles made up almost 10 percent of the population. If another facility has a lower truck frequency, one could change the parameters to give the long vehicles greater weight, since these vehicles would be more unique.

Although the example considered recurring congestion, it is reasonable to assume that vehicle movement within a queue should be similar regardless of whether the delay is recurring or due to an incident. Any deviations due to an incident, such as lane change maneuvers out of a blocked lane, would only serve to improve the response time of the algorithm. In fact, an incident during low flow conditions may cause an increase in lane change maneuvers without any measurable changes in local velocities or even the link travel time.

Although no effort was made in this algorithm to detect lane changes, an obvious extension would be to look across all upstream lanes rather than a single lane. Nonetheless, as demonstrated in this Section, the algorithm works using data from a single lane. One could also treat each lane as an independent process and integrate the results from all lanes for a more robust indicator. For example, if several adjacent lanes simultaneously showed a drop in the $ttR_0$ moving average, one could respond before any of them reached zero. On the other hand, if lane changes are frequent under free flow conditions, such as in a weaving section, one could map the normal pattern of movements. Then, for a given downstream observation, explicitly look in a different upstream lane. Future research will address these points and attempt to optimize the algorithm parameters, e.g., changing the minimum vehicle length, the travel time range(s), and the number of vehicles in the moving average.

As it stands, the algorithm has been running in real-time for over one year, across seven detector stations in the BHL. Although only a few hours of ground truth data have been generated, this long testing period has provided ample evidence of the algorithm's performance. Figure 3-10 shows an entire day's worth of travel time data from five lanes in one direction on a 0.5 km link. The algorithm's measurements are shown with dark points. The algorithm found the fewest matches in lane one[9] and the most in lane three, 542 and 2,100 matches, respectively. Throughout the entire day the algorithm gave consistent results across all five lanes. For reference, this

---

[8] The typical sampling period is on the order of 30 seconds in conventional practice.
[9] Due to a truck restriction, only 2 percent of all vehicles in this lane were long enough to be considered by the algorithm.

example uses the algorithm from Section 2 to match vehicles during congested conditions, as shown with light points.[10] It is worth noting that both algorithms were run throughout the entire day; each one is self-selecting, only matching vehicles when it can.

Obviously, it would be desirable to test the methodology at many locations. But the research has been constrained by the simple fact that most operating agencies do not collect data on individual vehicles. Conventional practice aggregates the measurements over fixed sample periods in the field.

### *3.7 Conclusions*

This Section has developed a new traffic surveillance strategy using existing detectors. Rather than reporting local conditions at the detectors, the strategy identifies periods when the link between two detector stations becomes congested. This process showed good performance over a 2.1 km segment with two ramps. Unlike most surveillance strategies that attempt to match vehicle measurements between detector stations, this work is compatible with the existing detector infrastructure. Perhaps more importantly, it is simple enough that it has been implemented using the existing Model 170 controllers, which are based on 20 year old computer technology. The key to this implementation is using the controllers to relay the data to a central server, as discussed in Section 4. For this limited deployment, the additional cost per station was roughly one percent of the cost for a new detector station. Presumably these costs would be even lower for a large scale deployment.

To place the work in context, the algorithm does have a lower reidentification rate than the other methods that require new hardware, but perhaps the higher rate is not necessary. One could view the algorithm as a low cost means to investigate the benefits of vehicle reidentification and travel time data before investing in a new surveillance system. In any event, the algorithm is intended to augment, rather than supplant, conventional point detector measurements. By combining point detector data with the new link data, it should be possible to identify transients in either data set and improve performance beyond what would be possible with just one of these data sets.

---

[10] Note that the total number of matches reported above does not include any matches from the second algorithm.

Figure 3-1, One vehicle traversing an extended link between two detector stations, illustrating the free flow travel time range. (A) The vehicle travels at a free flow velocity and it was observed at the upstream station during the time range; (B) the vehicle traveled slower than the minimum free flow velocity and it passed the upstream station before the start of the time range.

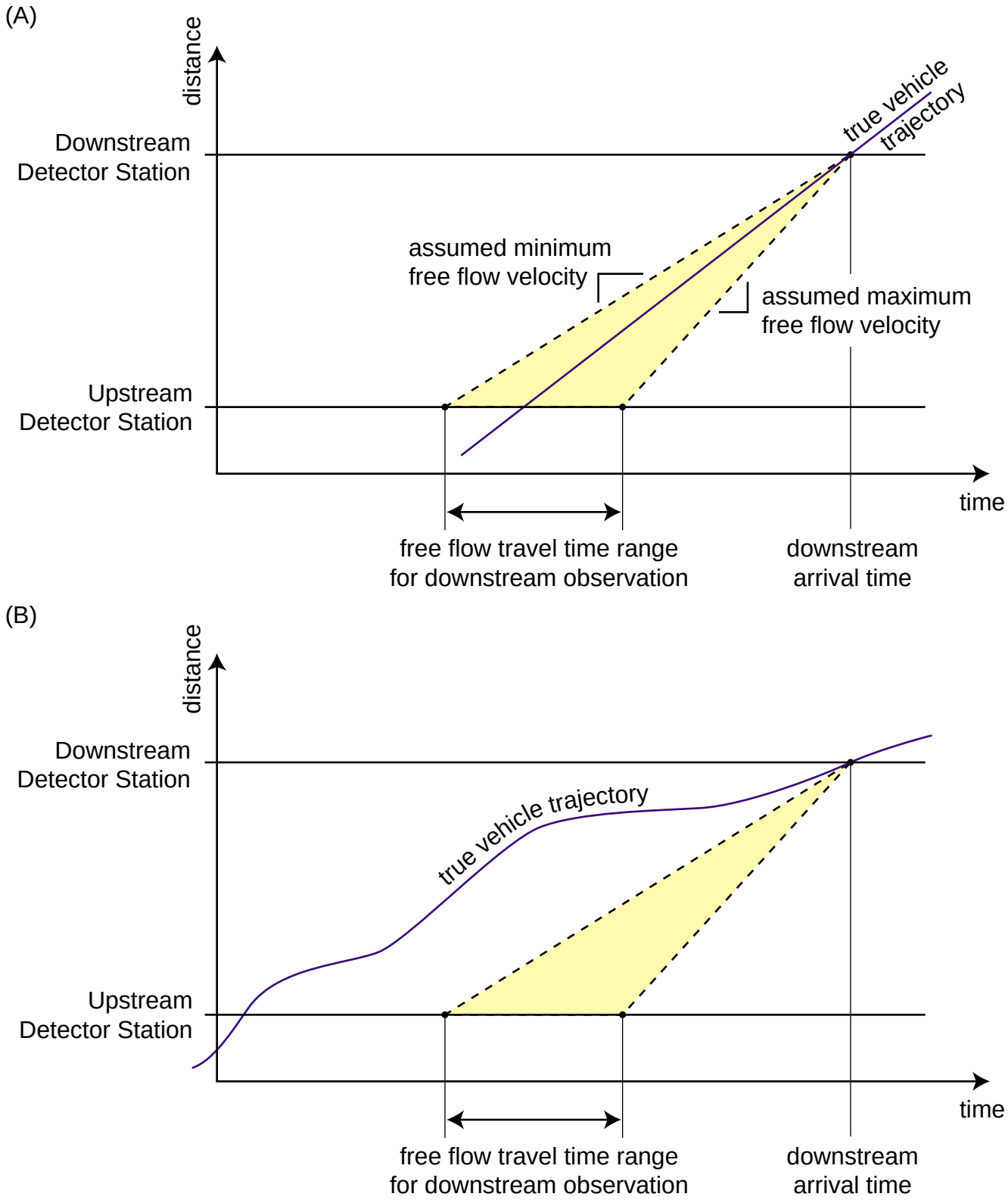

Figure 3-2, (A) Cumulative distribution of individual vehicle lengths over 24 hours at one detector station. (B) detail of part A.

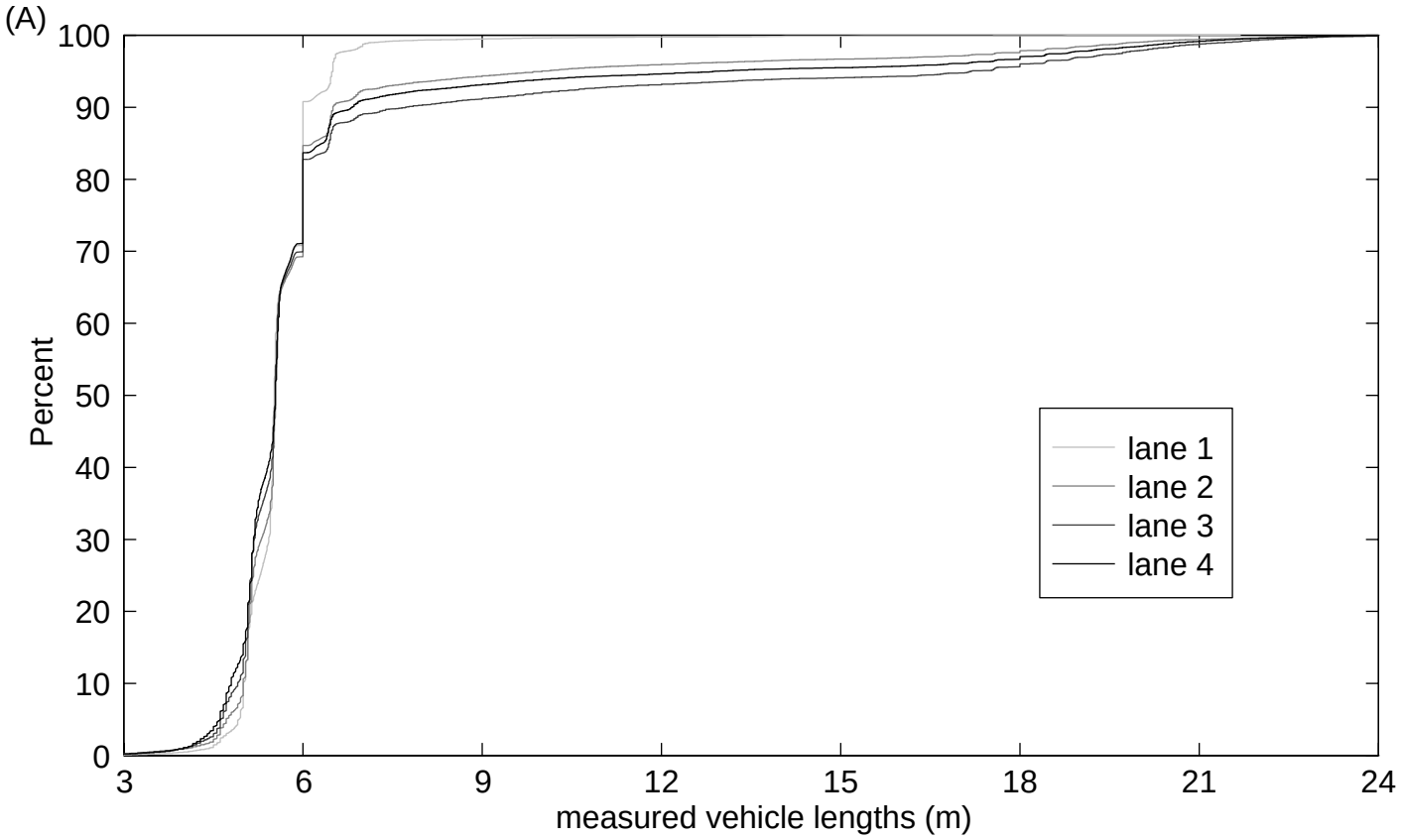


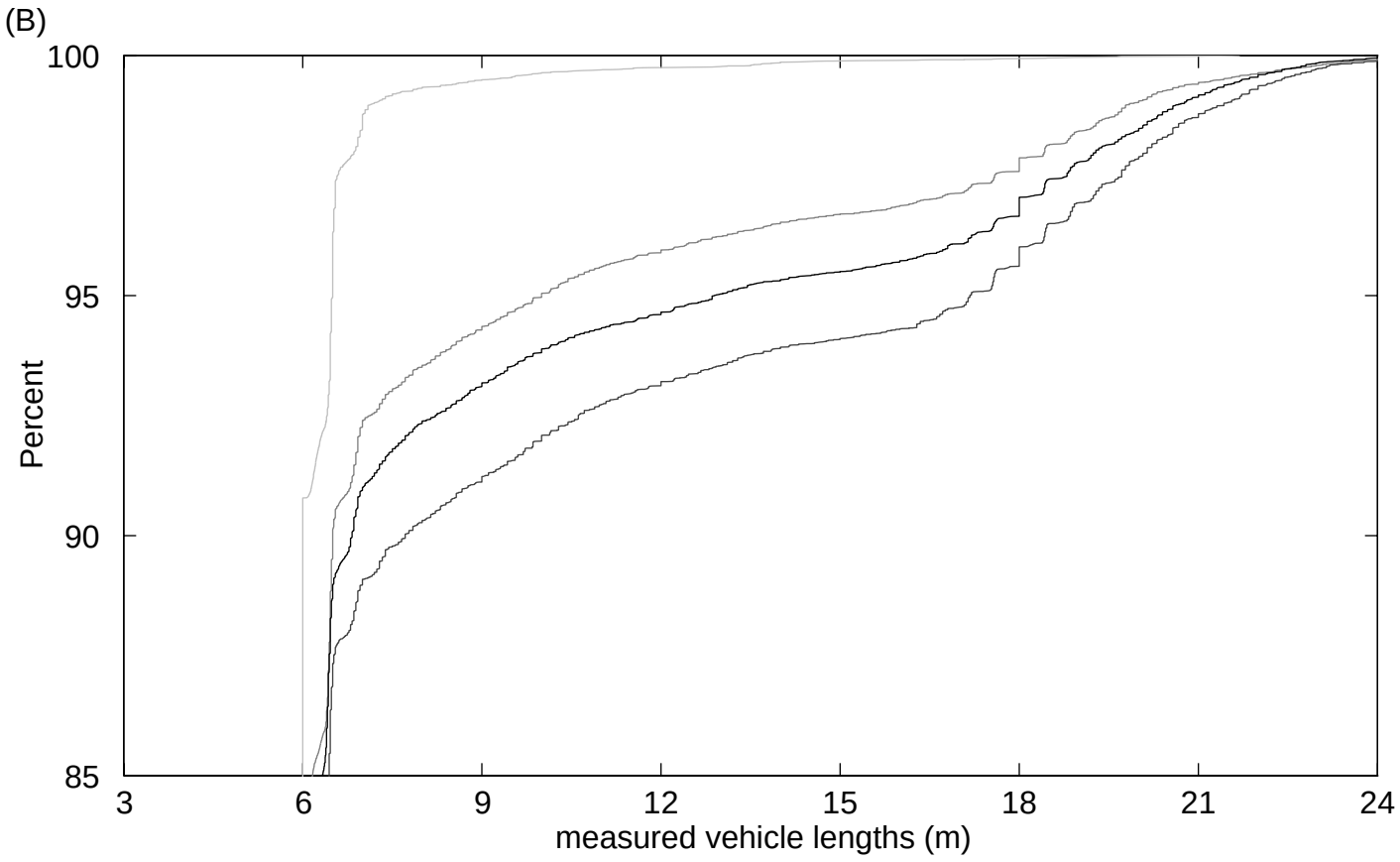

Figure 3-3, The segment of Interstate-80 in Berkeley, California used to illustrate and verify the Surveillance Algorithm.

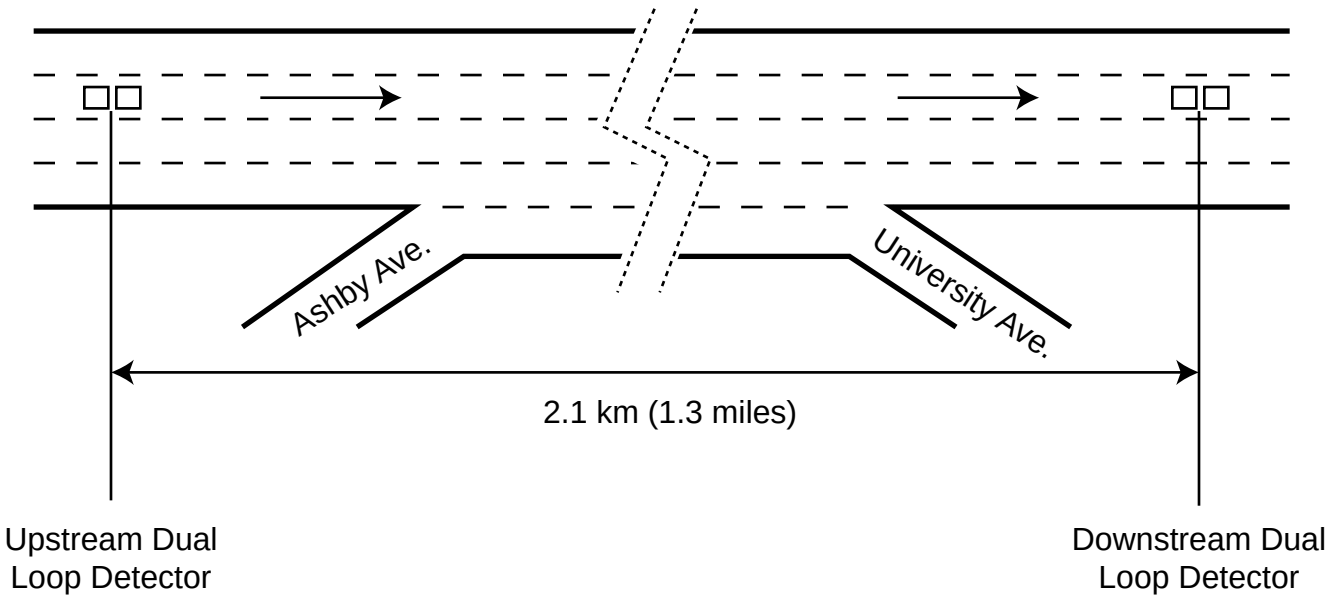

Figure 3-4, Each pair-wise test is assigned a value of 1 if a match is found and 0 otherwise. This plot shows the moving average of 10 sequential outcomes. There is a noticeable drop at 14.7 hours.

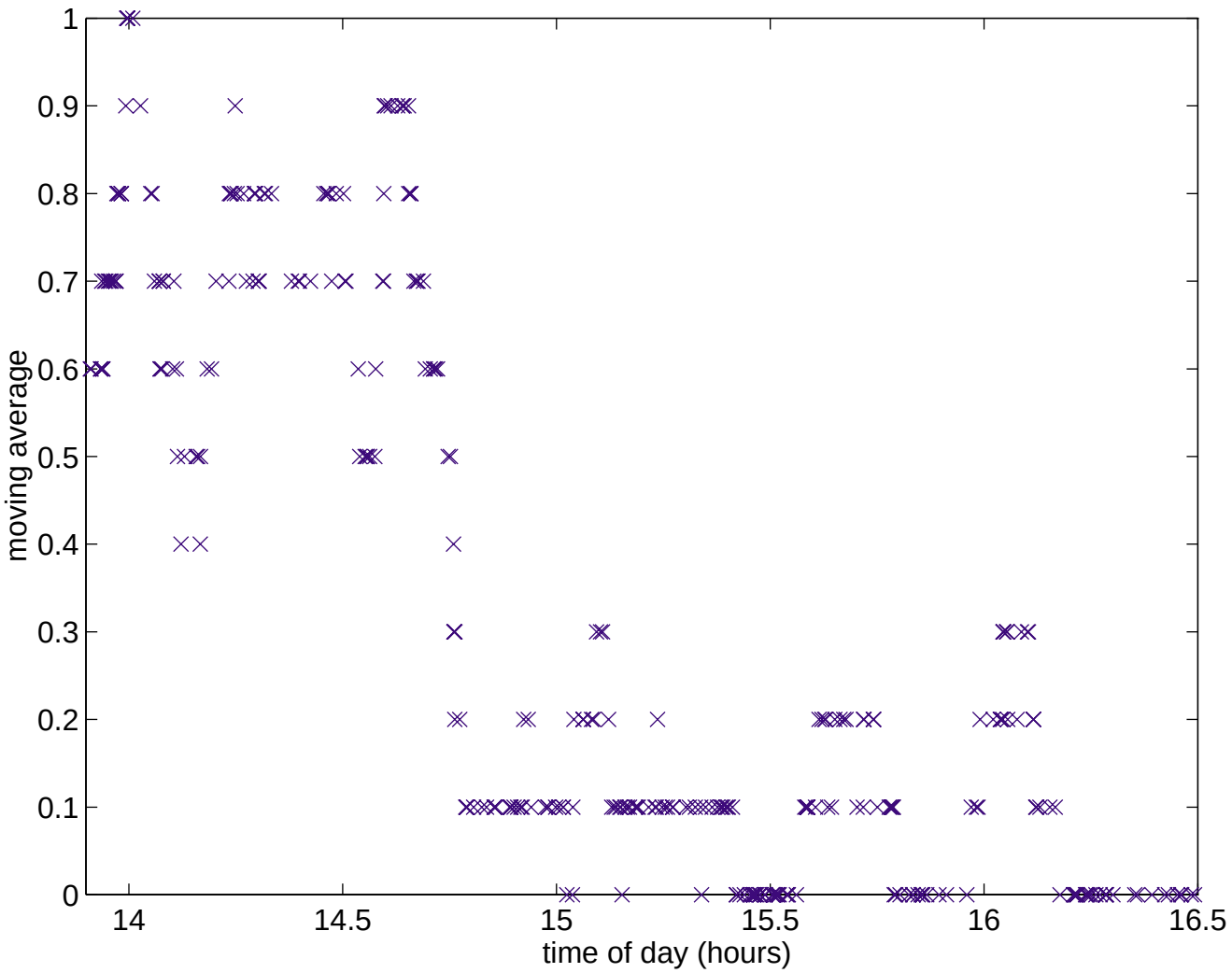

Figure 3-5, Measured travel times for matched vehicles ("fast matches") and ground truth travel times. Note that the algorithm did not find any matches after the true travel times increased due to congestion.

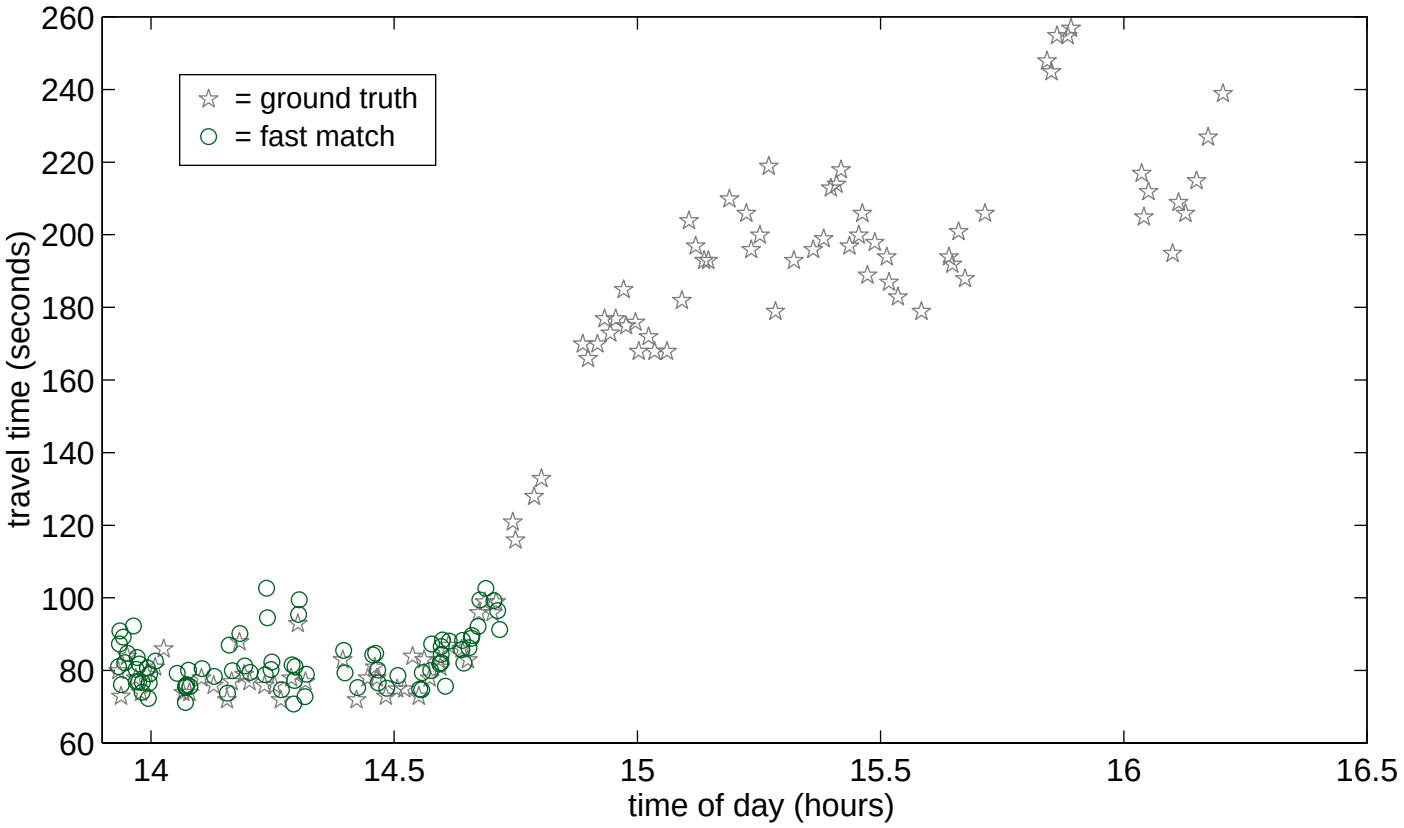

Figure 3-6, (A) The number of unmatched vehicles preceding each fast match. The free flow matches typically have few unmatched vehicles compared to the congested matches after 14.7 hours. (B) Moving sum of two measurements from part (A).

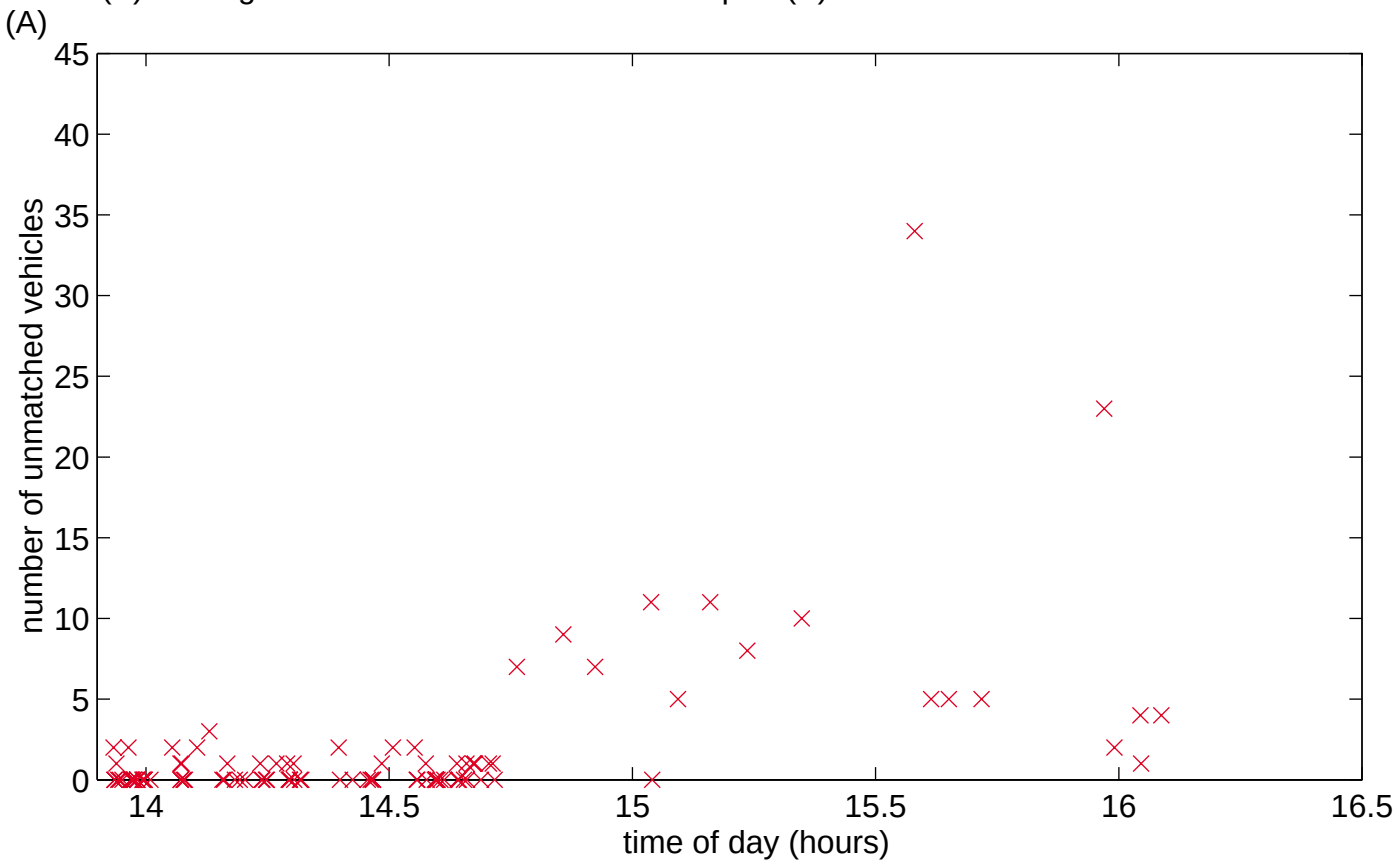


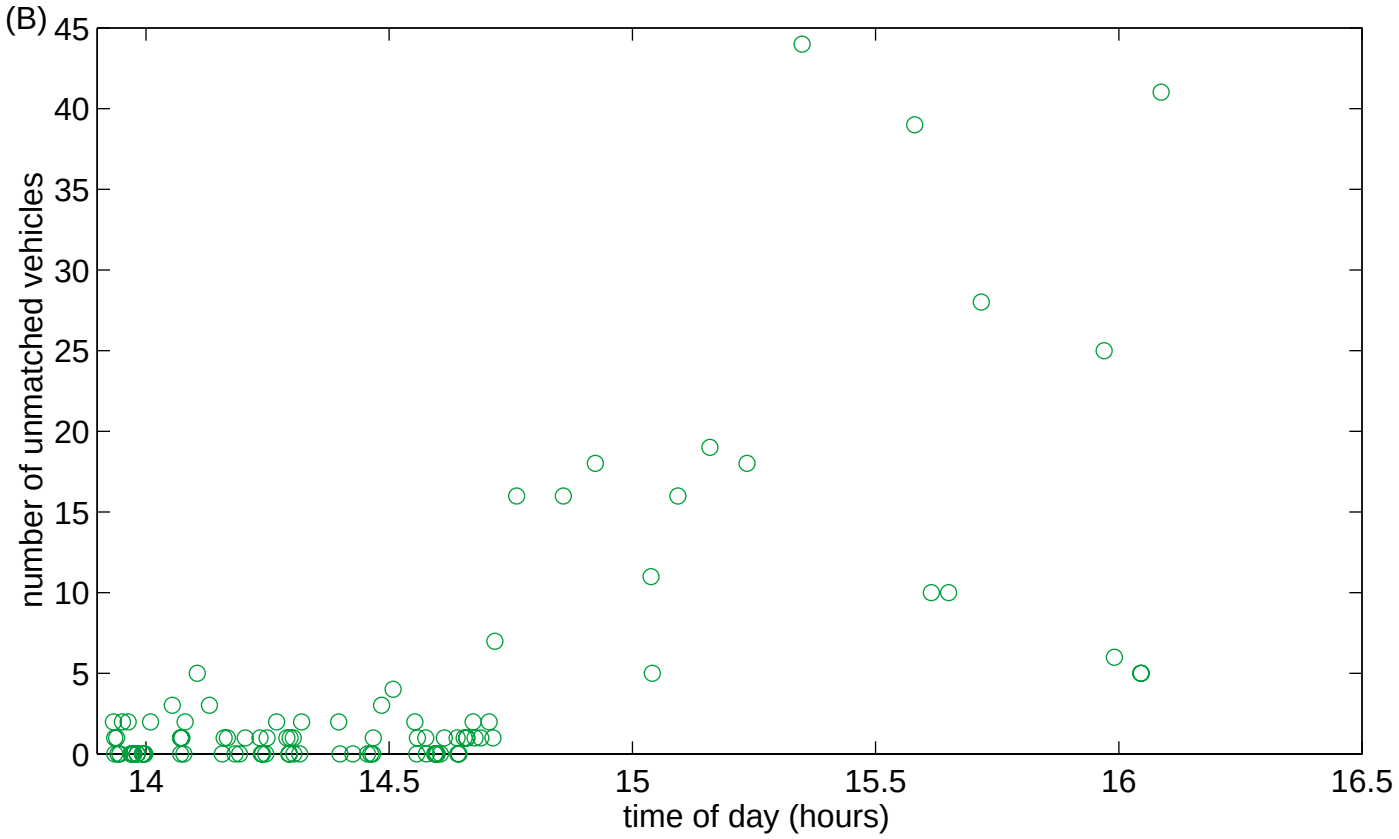

Figure 3-7, Discarding all matches preceded by a large number of unmatched vehicles before calculating the moving average, this plot yields a better contrast between free flow and congested conditions.

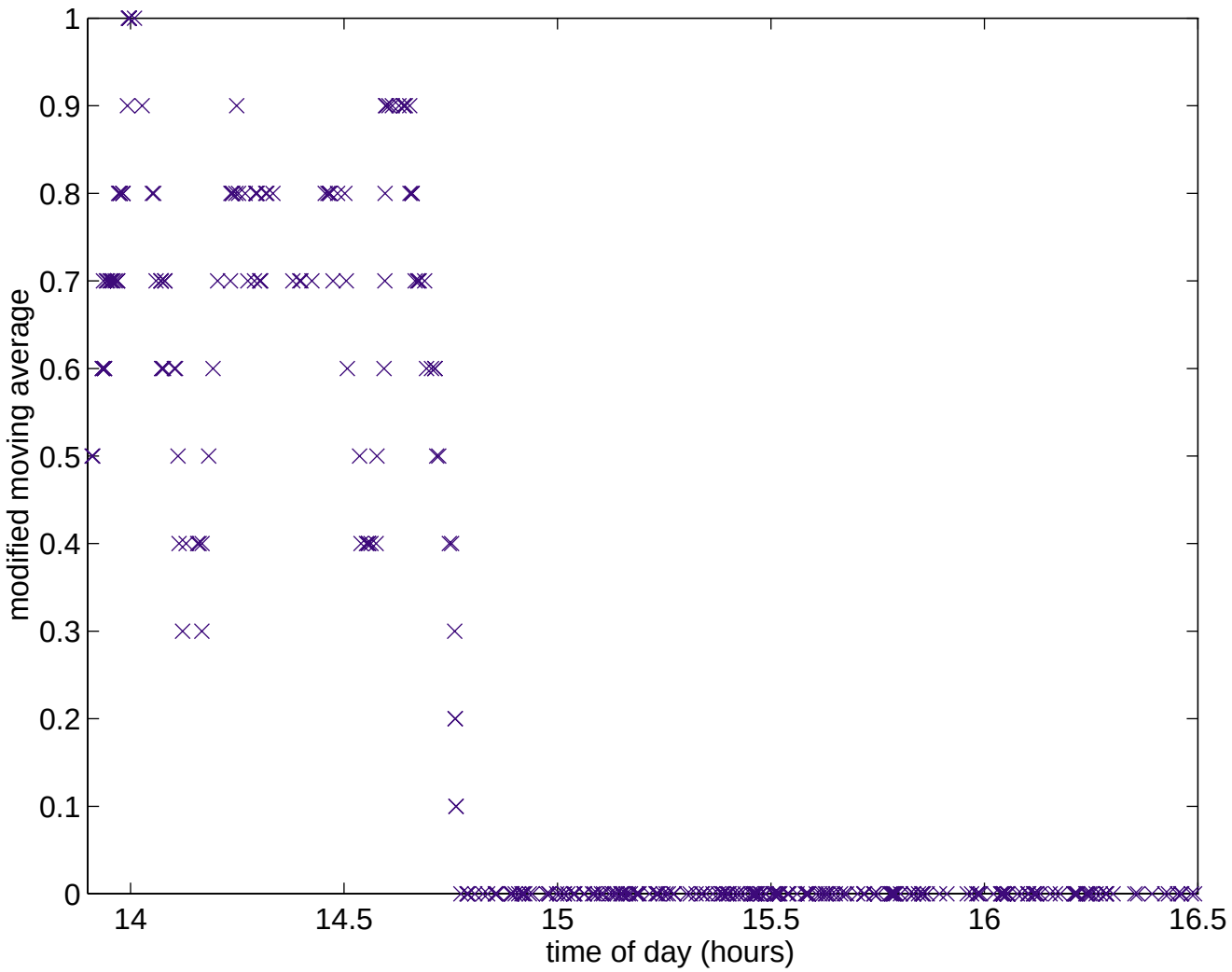

Figure 3-8, (A) Repeat the analysis from the preceding figure, for the first three time ranges. (B) Only accept non zero values for the new time ranges of the immediately faster range was non-zero at the start of the period. (C) Select the time range with the highest moving average at the given instant.

(A)

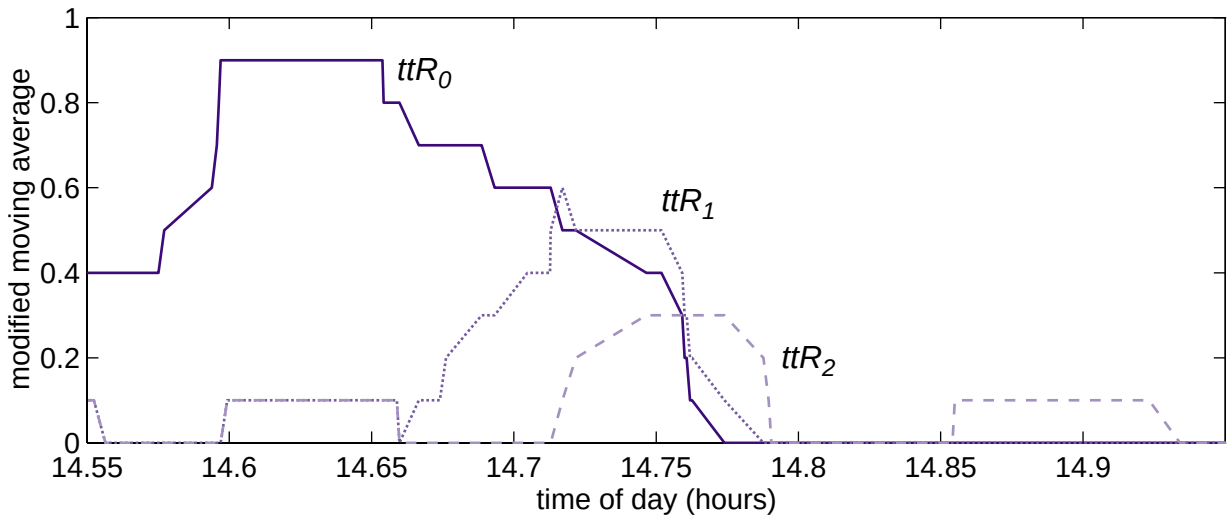


(B)

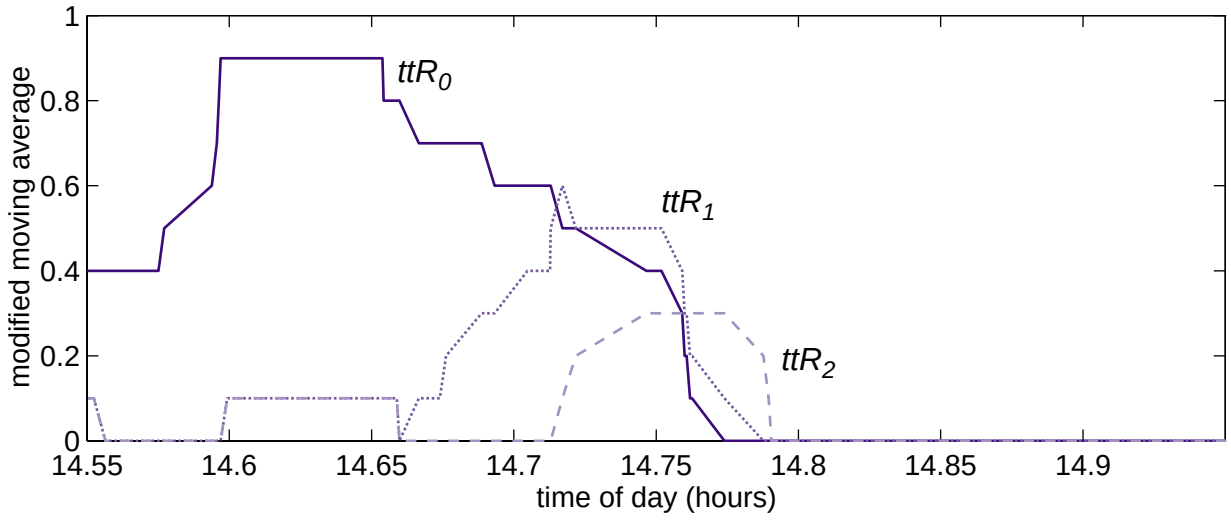


(C)

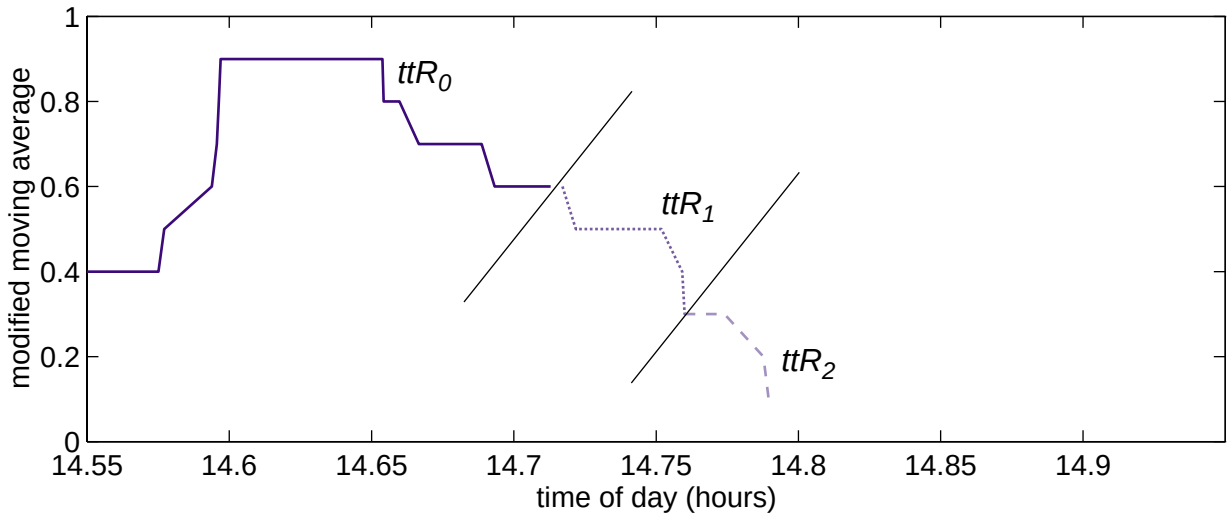

Figure 3-9, Measured travel times for matched vehicles from the five travel time ranges, as indicated, and the ground truth travel times.

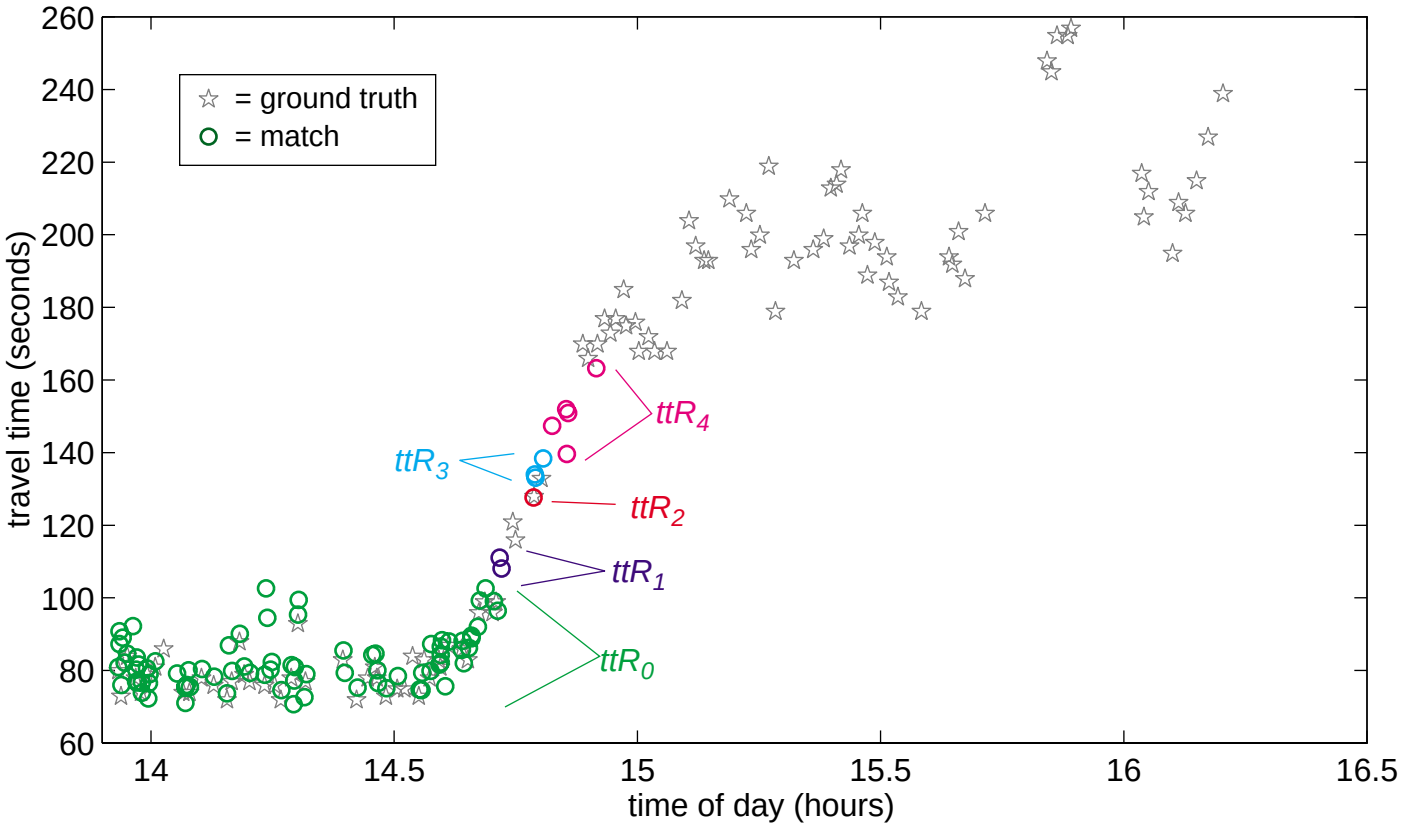

Figure 3-10, Measured travel time across five lanes over 550 m for an entire day using the algorithm in this paper (dark points) and a complementary algorithm during congestion (light points).

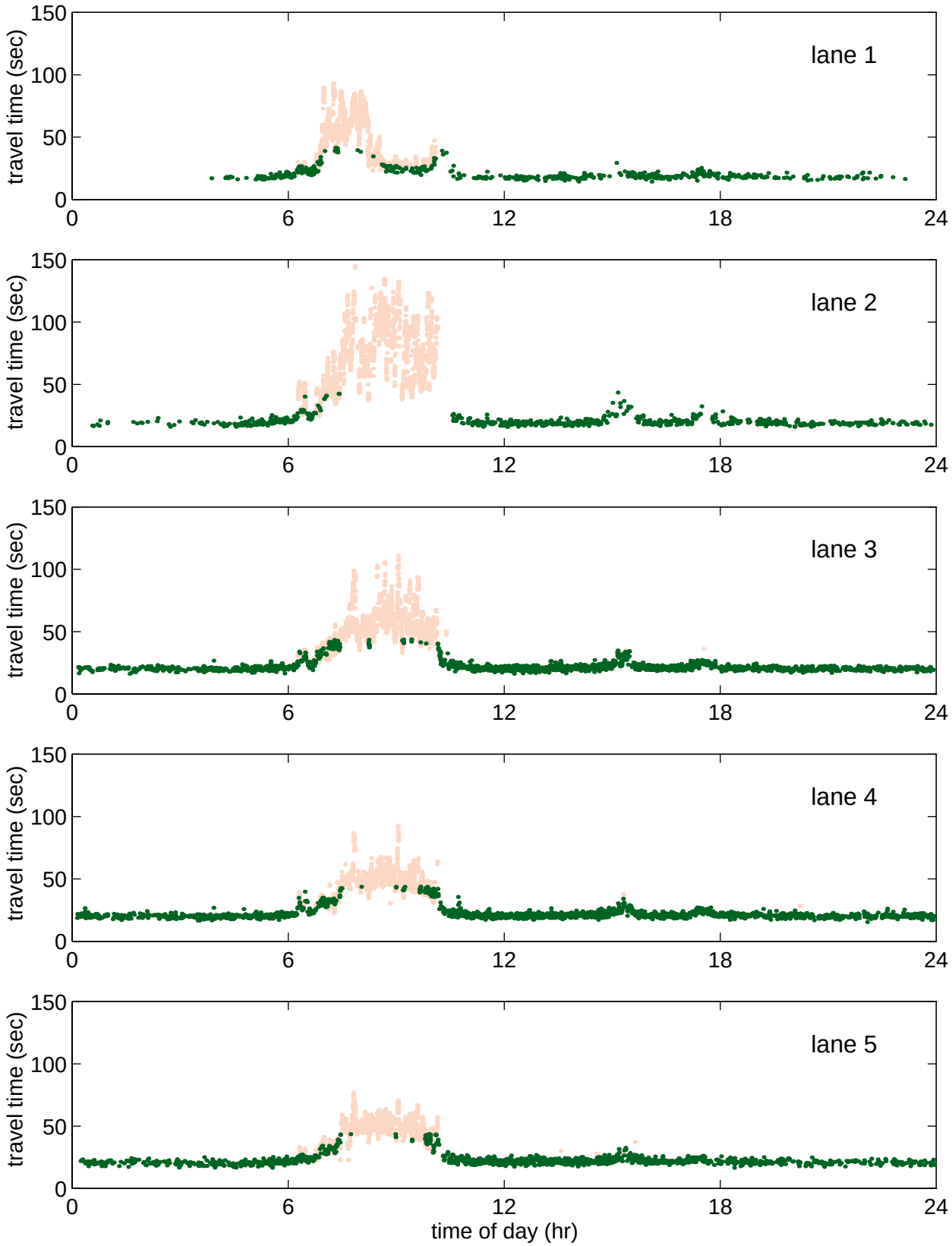

Table 3-1 The number of vehicles in various subgroups for the example.

| Subgroup | Size |
|---|---|
| total number of vehicles in the sample | 4344 |
| total number of long vehicles in the sample | 320 |
| number of ground truth matches | 106 |
| number of long vehicles before onset of congestion | 115 |
| number of fast matches | 82 |

# 4 THE BERKELEY HIGHWAY LABORATORY- BUILDING ON THE I-880 FIELD EXPERIMENT[11]

## *4.1 Introduction*

This Section presents the development of the Berkeley Highway Laboratory (BHL). Several goals underlie this development, including: collecting traffic data for research, extracting meaningful information from this data, furthering traffic flow theory and improving traffic control strategies. The laboratory represents the union of many researchers from the Departments of Civil Engineering, Electrical Engineering, Computer Science, and Statistics at the University of California, Berkeley (both past and present), as well as practitioners from the California Department of Transportation (Caltrans) (see Table 4-1 for a partial list of participants). The group has been meeting continuously since 1993 to work on a number of traffic related studies.

The first Subsection reviews preceding work that influenced the development of the BHL or that have been directly incorporated in the BHL. The next Subsection outlines the traffic surveillance component of the laboratory. Finally, this Section discusses the analytical component of the laboratory.

## *4.2 Preceding Work*

### 4.2.1 The I-880 Field Experiment

In 1993, members of the BHL group designed and implemented the I-880 Field Experiment to assess the benefits of Freeway Service Patrols. The Field Experiment collected peak period data from 19 detector stations equipped with dual loop speed traps, extensive incident data, and probe vehicle travel times for 50 week days. Rather than aggregating the detector data into discrete samples, the database contains event data (i.e., individual detector actuations) sampled at 60 Hz (Skabardonis et al., 1995, Skabardonis et al., 1996, Petty, 1995). Because the database is so rich and the fact that all of the data is available over the Internet, it has become one of the leading resources for traffic research around the world.

Many lessons were learned during implementation and subsequent analysis. The implementation itself was labor intensive, each day had up to five probe vehicles navigating the 14 mile round trip over the study region and each vehicle had two staff members. On the wayside, the existing

[11] A. Skabardonis and D. Lyddy helped prepare this Section.

communications infrastructure could not transmit the high resolution detector data, so this had to be collected manually. The database was sufficient to assess the benefits of Freeway Service Patrols, but it may not be detailed enough for other applications. For example, with only 50 days, the data set may not be sufficient for long term studies. Next, the data only includes peak periods and does not have any weekend data. The headway between probe vehicles may be too long to verify some applications. Finally, each probe vehicle and detector station had a clock, but these clocks were not coordinated accurately.

### 4.2.2 Machine Vision Vehicle Tracking

Other members of the BHL group have been working to develop machine vision based vehicle tracking tools and three distinct approaches have evolved from this work. The first approach finds the boundaries between vehicles and the background, then dynamically tracks and updates these closed contours from frame to frame (Koller et al, 1994a, Koller et al, 1994b). The second approach maintains a continuous update of the scene's background and subtracts this background estimate from each incoming image. The result of this subtraction is then thresholded to form "blobs" corresponding to vehicles. Each blob is tracked as a region using cross-correlation with dynamic updating. Both methods use a rudimentary occlusion reasoning algorithm to keep overlapping vehicle images separate; but both methods require that vehicles be separate when they are first detected, which is not always possible when traffic is heavy. Additionally, the performance of these trackers degrade significantly in the presence of long shadows.

The third approach was developed to improve the vision sensor's performance under all conditions. Rather than attempting to detect entire vehicles, this system locates and tracks corners of vehicles. The history of these tracks is then examined by a grouping algorithm, which uses common motion and proximity cues to group sets of tracks into vehicle hypotheses (Beymer et al., 1997, Coifman et al., 1998). The advantage of this feature tracking over other tracking strategies is that a given vehicle can be correctly detected and counted as long as at least one feature remains visible throughout the entire tracking region. This fact makes feature tracking more robust in the presence of occlusion. Figure 4-1A-B show the results of (A) feature tracking and (B) grouping for two typical sequences; while Figure 4-12C is a plot of several tracker-generated vehicle trajectories (solid lines) along with ground truth (dashed). The ground truth in this figure was generated by a human observer who scrolled through the image sequence and manually marked each vehicle's position. By definition, the slope of each trajectory is simply the given vehicle's velocity at that instant and the horizontal trajectories represent vehicles which have stopped. This figure shows that, unlike most tracking systems, the feature tracker was able to follow vehicles even if they stop momentarily. Finally, note that this plot only shows the distance along the

roadway, the tracker also extracts the lateral position, so it is a trivial matter to identify lane changes within the surveillance region.

### 4.2.3 Link travel time (LTT) measurement

The BHL group has looked at many applications of traffic data, highlighting one of these applications, we have developed three different approaches for calculating LTT. The first approach (Petty et al., 1998) used an empirical semiparametric model for the LTT distribution, which is assumed locally time-invariant. Each sensor measures a cumulative arrival pattern; since each vehicle is modeled as picking its travel time i.i.d., the downstream pattern is given by the upstream pattern convolved with the LTT distribution. A method of moments analysis allows the extraction of the maximum-likelihood travel time distribution from the observed data. This approach proved quite effective in practice when tested on the I-880 loop data.

The second approach (Huang and Russell, 1997) tried matching individual vehicles in order to find both LTT and O/D counts. This work used vehicle features extracted by the video tracker, including arrival time, position, speed, color, and size. Vehicle reports from two successive camera sites were *matched* using a combinatorial matching algorithm that computes the probability that a proposed match between two vehicle observations is correct. The system reported as matches any proposed match whose probability exceeded a prespecified threshold on accuracy. With an accuracy threshold of 50 percent, the algorithm was able to match 80 percent of vehicles in a test sequence. With an accuracy threshold of 90 percent, it was able to match 15 percent of the vehicles. Even with such low coverage, the estimated travel time was accurate to within one percent.

The third approach, presented in Sections 2 and 3, reidentifies vehicles using effective vehicle lengths measured at dual loop speed traps. This approach uses the existing detector and controller hardware to extract a vehicle signature. The basis for this approach is recognizing the fact that the sequence of measured lengths in a platoon provides more information than do the individual measurements. The algorithm was rigorously tested over two sample sets, with a net total over 1,400 vehicles. It matched approximately 60 percent of the vehicles with LTT measurement errors ranging between 0 and 5 percent.

## *4.3 BHL Traffic Surveillance*

Work is underway to develop the surveillance portion of the BHL on Interstate 80, just north of Oakland, California, as shown in Figure 4-2. The site includes eight dual loop speed trap detector stations along the freeway and 14 video cameras on top of the 30 story Pacific Park Plaza. Because

of a downstream bottleneck, the westbound traffic (compass southbound) at this location is typically congested for over ten hours during any given weekday. The following provide more detail about the loop detectors, video surveillance system, and video based vehicle tracking.

### 4.3.1 The Loop Detectors

The standard Caltrans detector station uses a Model 170 controller sampling the loop sensors at 60 Hz. Under normal operation, the 60 Hz event data are internal to the controller, and the output data are typically aggregated into 20 second or 30 second average velocity, flow, and occupancy measurements. Caltrans developed new controller software for the I-880 Field Experiment that preserves the 60 Hz event data. Because the Model 170 controller is based on 20 year old technology, simply outputting this data stream consumes all of a controller's processing power. The I-880 Field Experiment used a laptop computer, in conjunction with each controller, to collect and store this data stream in the field. The BHL uses the same controller hardware and software, but rather than storing the event data locally in the controller cabinets, it is transmitted to campus via a wireless modem and the Internet. Figure 4-3 shows an overview of the communications system. The controller generates a new data packet each second. An inexpensive PC *client* is placed in each controller cabinet to collect the data packets, manage communications and relay the packets to a central server on campus. Once a packet has been sent, the client waits for an acknowledgment from the server. If no acknowledgment is received in a fixed period of time, the client resends the packet. It is worth noting that the additional hardware cost per station is less than one percent of the cost to install a detector station for conventional traffic surveillance.

The remote data collection system eliminates the need to manually collect the detector data. All of the clients automatically reset their clocks to the same reference each day at approximately 3:00 AM; thereby eliminating any clock discrepancies between stations. Finally, the I-880 Field Experiment was constrained by limited storage capacity on the circa 1993 laptops, as a result, data collection was restricted to weekday peak periods. In contrast, the new laboratory uses a central server with enough disk space to store over 1,000 hours of data from each station in the BHL. The database is periodically backed up to CDROM, thus, allowing the new system to monitor the freeway continuously, 24 hours a day, seven days a week, indefinitely.

### 4.3.2 Video Surveillance System

As previously noted, the I-880 Field Experiment has relatively long headways between successive probe vehicles. The new laboratory utilizes 12 fixed mount video cameras to overcome this

problem, thus allowing any vehicle to serve as a probe. Two additional cameras are remotely controllable "Pan-Tilt-Zoom" (PTZ) units.

The fixed cameras are deployed to provide continuous coverage of the freeway, with one camera's surveillance region overlapping the next. These regions have been selected to optimize automated vehicle tracking from each camera's view. These cameras are connected to studio-grade video tape recorders (VTR's), housed on top of the Pacific Park Plaza, using S-Video format. The S-Video format provides physical separation of color and grayscale signals, allowing for better color constancy than standard composite video, which improves color-based matching. The VTR's record the S-Video signals on S-VHS tapes. The S-VHS format allows for highter bandwidth analo recording, which improves image clarity over standard VHS. This improved clarity leads to more accurate vehicle detection and localization.

The VTR's are capable of recording in several linear and time-lapse modes, ranging from the conventional 30 frames per second to a single frame per second. The VTR's will normally be set to record at five frames per second, which is sufficient for vehicle tracking and allows a standard T-120 tape to store 12 hours of video. In practice, the 12 hours will typically be divided to cover both morning and afternoon commutes. Tapes will be collected and replaced each weekday between the commute periods, and this intensive surveillance will last six to 12 months.

Finally, the PTZ cameras will allow for remote monitoring of the freeway. The video signals from the PTZ cameras will be fed through an on-site computer that will digitize, store, and forward the video frames to a campus-based web server via wireless Ethernet. This link has sufficient bandwidth for two video streams. The web server will also route control commands back to the on-site computer for remote control of the PTZ cameras and the VTR's.

### 4.3.3 Video Based Vehicle Tracking

Until now, video sensors and loop detectors have been widely regarded as competing technologies for traffic surveillance. Recognizing the fact that each detection system has strengths and weaknesses, the BHL work considers video and loops to be complementary. Loop detectors are widely available, perform under all weather and lighting conditions, and have been refined though several decades of deployment. In contrast, video sensor algorithms provide nearly continuous vehicle trajectories and a large set of features for vehicle reidentification.

Previous work by this group used loop data to verify video sensor performance (Beymer et al., 1997, Coifman et al., 1998) as well as using video to manually verify matches generated by loop based LTT algorithms. The BHL extends this combination of data beyond simple cross-verification

by coordinating loop and video data at the vehicle detection and tracking stage. This sensor fusion will yield data sets with the count accuracy of loop detectors and the spatially rich vehicle trajectories of video sensors. These higher quality data sets will in turn allow analysis algorithms to provide a better understanding of both microscopic driver behavior and macroscopic traffic flow. In addition, by comparing data generated by either sensor in isolation to fused data from both sensors, it will be possible to establish the performance tradeoffs one makes when deploying either type of sensor in the field.

## *4.4 BHL Analysis*

Several applications are being developed in conjunction with the BHL. This Subsection presents three of them: Real Time Travel Time Measurement, Understanding Traffic Flow and Improving Traffic Models, and Incident Management.

### 4.4.1 Real Time Travel Time Measurement

The first application of the BHL surveillance system is measuring travel times in real time. The LTT measurement system reidentifies vehicles from length measurements and is based on the algorithms presented in the previous Sections. Figure 4-4A shows an example of travel time measurements across one link, from one lane, over a 24 hour period. This work should help answer questions such as:

- What additional information does travel time provide in real time?
- What are the best ways to integrate this information with traffic management tools?

The lessons learned from this effort will help guide future investments in LTT measurement technology, as well as investments in conventional surveillance technology.

A partial answer to the first question is shown in Figure 4-4B, which indicates measured link density. A measurement is made whenever a vehicle is reidentified at the downstream detector. The value is the quotient of the total number vehicles to pass the upstream detector during the period that the reidentified vehicle traversed the link divided by the length of the link. The real time system can be viewed at: http://www.its.berkeley.edu/projects/freewaydata.

### 4.4.2 Understanding Traffic Flow and Improving Traffic Models

Most of the current traffic flow theories and models are based on limited empirical data because of the technology limitations in detailed data acquisition and processing. Furthermore, data processing and analysis techniques have been too limited to deal with large amounts of data. The end result is that observed traffic phenomena cannot be well correlated with the interactions of individual vehicles and how they relate to design and control characteristics.

For example, limited information is available on the operation of freeway merging and weaving areas that involve intense vehicle interactions and lane-changing maneuvers over a restricted distance. Although previous studies videotaped the operation of merging/weaving areas, the recordings were not analyzed microscopically (i.e., vehicle trajectories) to gain a better understanding of vehicle interactions. Additionally, most measurements and analyses are focused on the segment (link) of interest, without satisfactorily considering the spatial and temporal impacts in the network.

The tools developed in conjunction with the BHL for combining, processing and analyzing data from video and loop detectors will provide the basis for better understanding traffic flow and developing improved models. The focus here is not merely to discuss "*what is happening*", but to formulate improved models and consequently predict the impacts of ATMS, ATIS or other scenarios.

### 4.4.3 Incident Management

Previous research on incidents have either tried to quantify the problem or develop rapid detection schemes. The effectiveness of incident management measures has been based on simplified techniques with several assumptions about incident impacts to traffic flow. Although countless automated incident detection strategies have been proposed, most of these systems suffer from high false alarm rates and/or long detection times.

A novel analysis framework for estimating the benefits of detection/management strategies was developed by the BHL group and is illustrated in Figure 4-5. Rather than considering a single facet of incidents, the analysis framework considers the complete system: expected costs from incidents, costs for given levels of detection reliability and costs from mitigations, Petty et al., 1999.

Using the surveillance tools described above, members of the BHL group will proceed systematically to develop an improved incident management strategy. For example, construct semi-empirical models of the effect of the occurrence of incidents on the evolution of travel times at

neighboring points, combine this information with historical models of the relation between data from other sources and incidents, then estimate the probability of an incident given the data.

Given such probability information, we can carry out a utility-directed analysis to compute an optimal policy for responding to suspected incidents. It should be possible to set the "incident detector threshold" to such a level that the value of responding to detected events (e.g., by tow-truck dispatch and changeable message signs) outweighs the cost of false positives. This work should yield the nature and extent of the sensor data required to make emergency response substantially beneficial.

### *4.5 Conclusions*

This Section has given an overview of the BHL, starting with preceding studies that have influenced or that have been incorporated into the laboratory. The first Subsection discussed the surveillance components of the BHL, which include event data from dual loop speed traps, extensive video surveillance data, and accurate vehicle trajectories automatically extracted from combined loop and video data. The Section closes by presenting some of the analytical components in the BHL. The laboratory will be used to demonstrate real time LTT measurement using existing vehicle detectors. The lessons learned from this effort will help quantify the true benefits of LTT data and help guide future investments in traffic surveillance technology. The accurate vehicle trajectories should lead to a better understanding of traffic flow and they will be used to improve traffic models. This work should allow for significant advances over previous studies that only relied on point detector data and/or information manually extracted from videotapes. Finally, the Section discusses a new approach to incident detection and management. Rather than considering a single facet of incidents, this work considers the complete system: expected costs from incidents, costs for given levels of detection reliability and costs from mitigations.

Figure 4-1, Vehicle tracking, (A) feature tracks (B) feature groups (C) Sample vehicle trajectories as a shock wave passes through the surveillance region (dashes = manually generated ground truth, solid = tracker output)

(A)

(B)

(C)

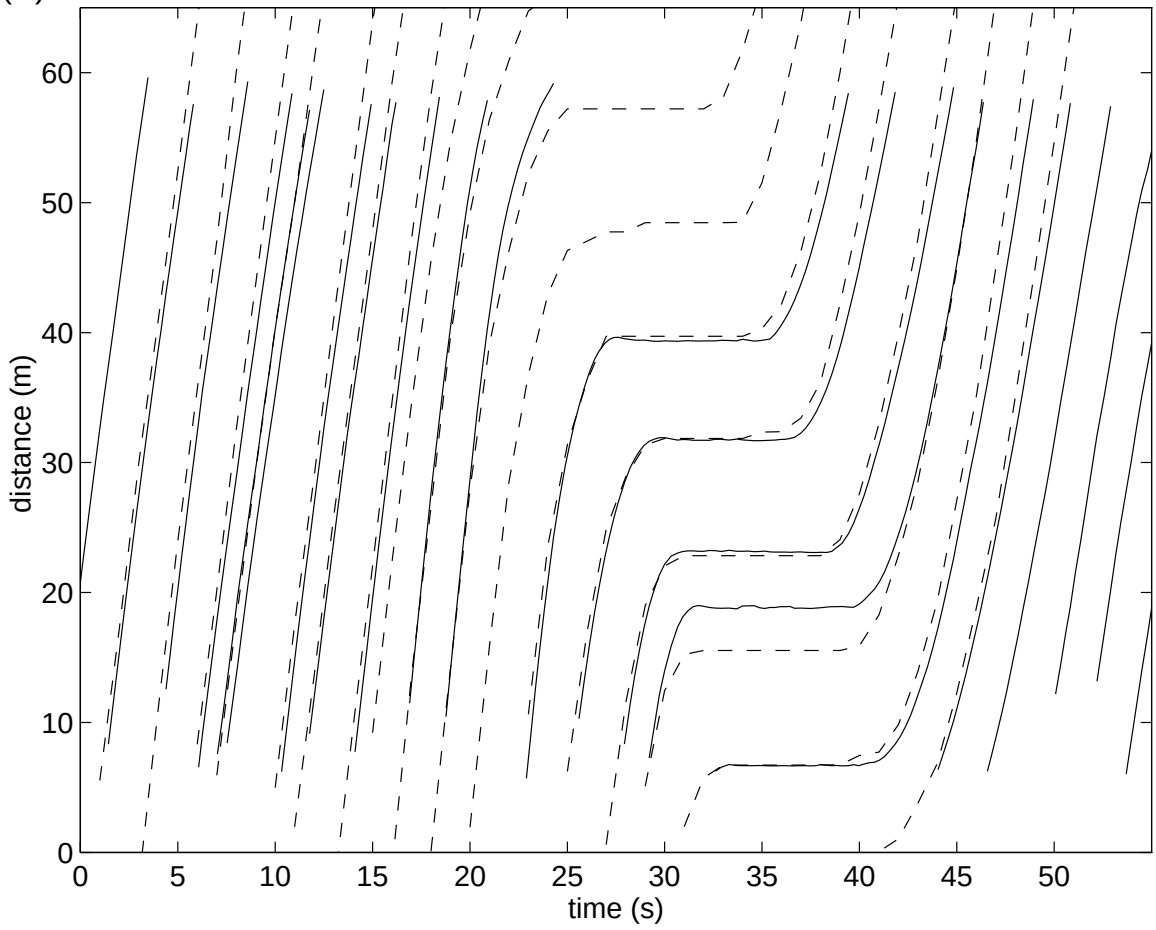

Figure 4-2, The Berkeley Highway Laboratory surveillance site. The site includes eight dual loop speed trap detector stations along Interstate 80 and 12 video cameras on top of the 30 story Pacific Park Plaza, just a few feet off of the edge of pavement.

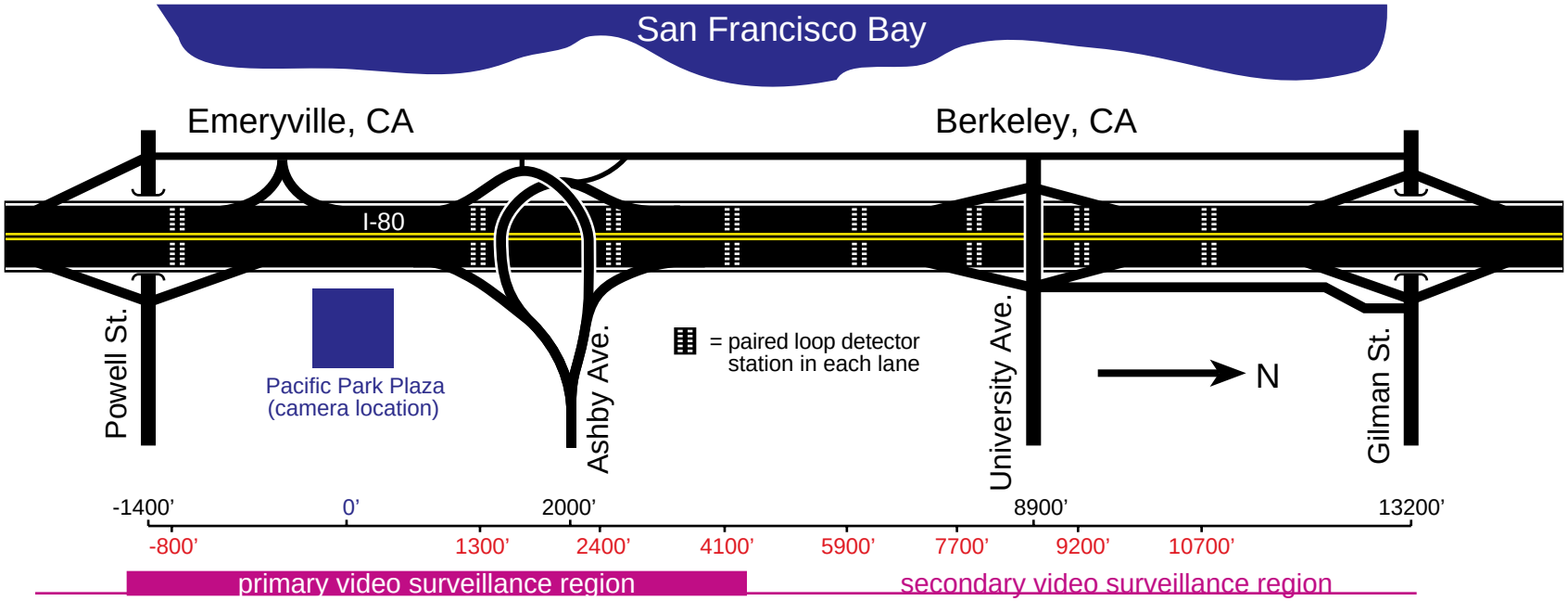

Figure 4-3, Communications overview showing the data stream from the detectors to campus.

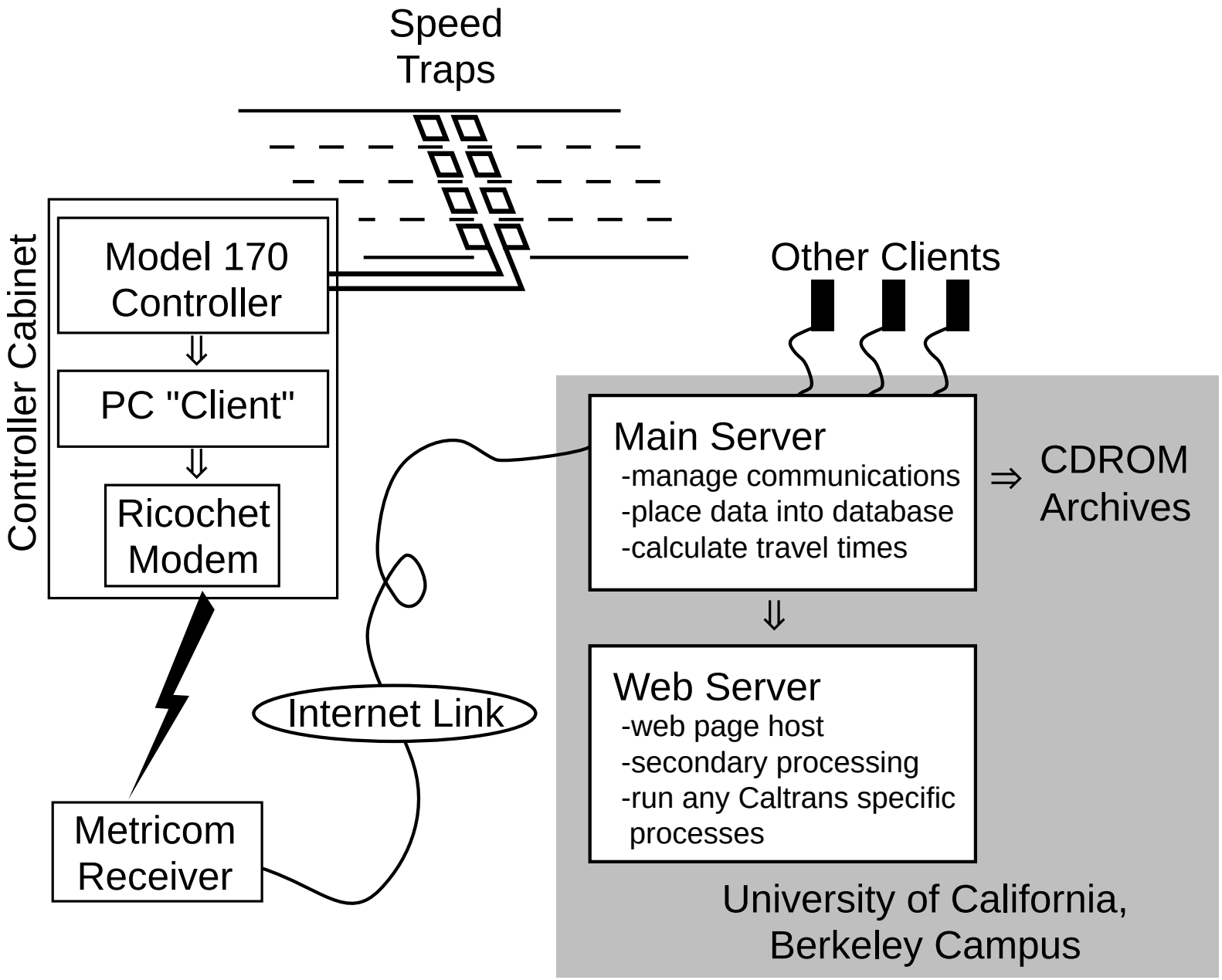

Figure 4-4, (A) Measured link travel times over a 24 hour period for one lane of one link in the BHL. (B) The corresponding link densities.

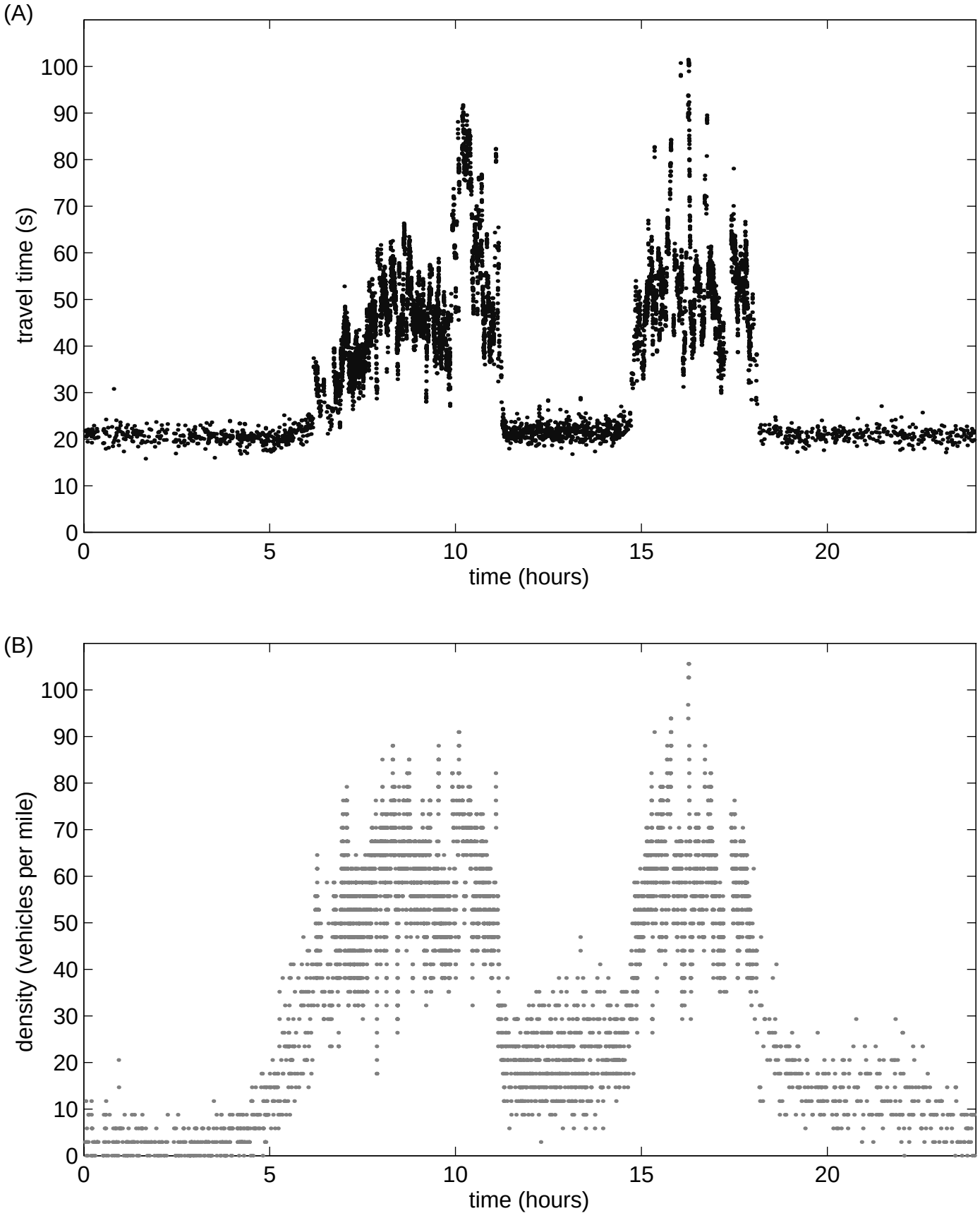

Figure 4-5, Schematic of the analysis framework for estimating the benefits of incident detection/management strategies.

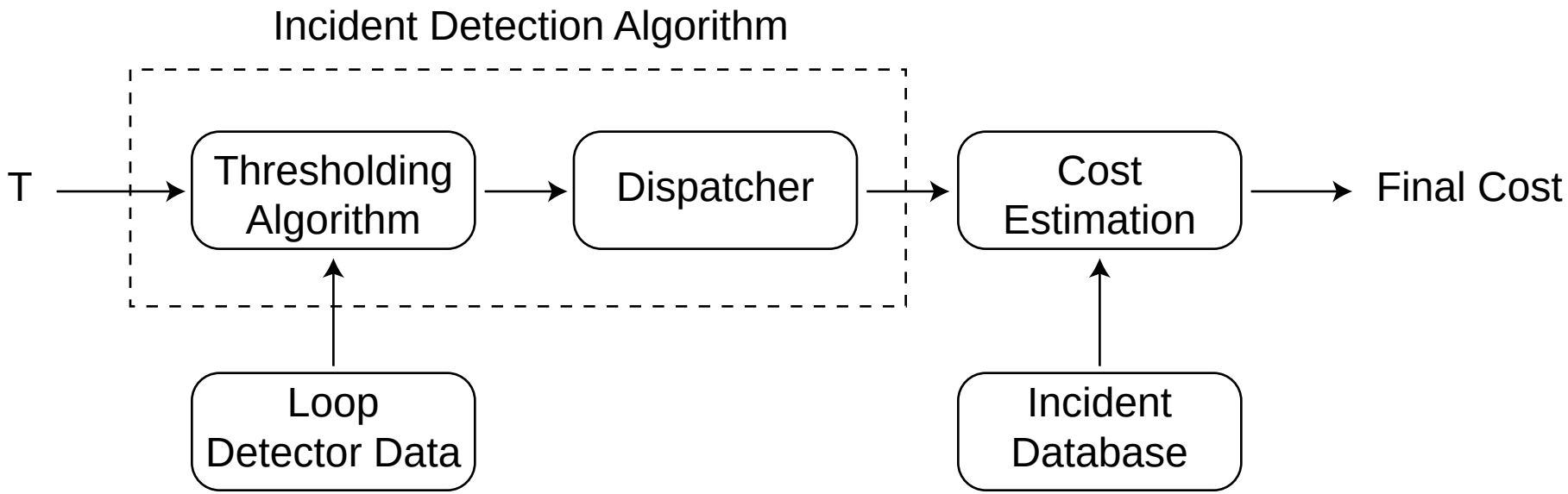

Table 4-1, A partial list of researchers and practitioners involved with the Berkeley Highway Laboratory.

| Participant | Affiliation |
|---|---|
| Bickel, P. | Statistics |
| Chen, C. | Electrical Engineering |
| Chen, J. | Caltrans |
| Chen, L. | Caltrans |
| Coifman, B. | Civil Engineering and Electrical Engineering |
| Coughlin, S. | Caltrans |
| Friesenhahn, M. | Statistics |
| Huang, T | Computer Science |
| Kwon, J. | Statistics |
| Lyddy, D. | Electrical Engineering |
| Malik, J. | Computer Science |
| Ostland, M. | Statistics |
| Palen, J. | Caltrans |
| Petty, K. | Electrical Engineering |
| Rice, J. | Statistics |
| Russell, S. | Computer Science |
| Skabardonis, A. | Civil Engineering |
| Varaiya, P. | Electrical Engineering |
| Zhang, X. | Statistics |

## 5 ACKNOWLEDGMENTS

The authors would like to acknowledge the input, contributions and support from Alexander Skabardonis, Mike Cassidy, Daniell Lyddy, Randall Cayford, Edgar Ergueta, and Gabriel Gomes at the University of California, Berkeley, as well as Joe Palen, Sean Coughlin, Ron Slade, and Judy Chen at Caltrans.

# 6 REFERENCES

Balke, K., Ullman, G., McCasland, W., Mountain, C., Dudek, C., (1995) *Benefits of Real-Time Travel Information in Houston, Texas*, Southwest Region University Transportation Center, Texas Transportation Institute, College Station, TX.

Beymer, D., McLauchlan, P., Coifman, B., and Malik, J., (1997) A Real Time Computer Vision System for Measuring Traffic Parameters", *CVPR97*, pp 495-501.

Chang, G., Kao, Y., (1991) An Empirical Investigation of Macroscopic Lane-Changing Characteristics on Uncongested Multilane Freeways, *Transportation Research- Part A*, Vol 25A, No 6, pp 375-389.

Coifman, B., Beymer, D., McLauchlan, P., and Malik, J. (1998) A Real-Time Computer Vision System for Vehicle Tracking and Traffic Surveillance, *Transportation Research: Part C*, vol 6, no 4, pp 271-288.

Coifman, B., (1998a) *Vehicle Reidentification and Travel Time Measurement Using Loop Detector Speed Traps*, Dissertation, University of California.

Coifman, B., (1998b) Vehicle Reidentification and Travel Time Measurement in Real-Time on Freeways Using the Existing Loop Detector Infrastructure, *Transportation Research Record 1643*, Transportation Research Board, pp 181-191.

Coifman, B., (1999) Using Dual Loop Speed Traps to Identify Detector Errors, *Transportation Research Record no. 1683*, Transportation Research Board, pp 47-58.

Coifman, B. (2001) Estimating Travel Times and Vehicle Trajectories on Freeways Using Dual Loop Detectors, *Transportation Research: Part A*, [forthcoming].

Cui, Y., Huang, Q., (1997) Character Extraction of License Plates from Video, *Proc. 1997 IEEE Computer Society Conference on Computer Vision and Pattern Recognition*, IEEE, pp 502-507.

Dailey, D., (1993) Travel Time Estimation Using Cross Correlation Techniques, *Transportation Research-Part B*, Vol 27, No 2, pp 97-107.

Holdener, D., Turner, S., (1996) Probe Vehicle Sample Sizes for Real-Time Information: the Houston Experience, *Intelligent Transportation: Realizing the Benefits- Proc. of the 1996 Annual Meeting of ITS America*, Vol 1, ITS America, pp 287-295.

Huang, T., Russell, S., (1997) Object Identification in a Bayesian Context, *Proceedings of the Fifteenth International Joint Conference on Artificial Intelligence (IJCAI-97)*, Nagoya, Japan. Morgan Kaufmann.

Koller, D., Weber, J., Huang, T., Malik, J., Ogasawara, G., Rao, B., and Russell, S., (1994a) Towards Robust Automatic Traffic Scene Analysis in Real-Time, *ICPR94*, pp A:126-131.

Koller, D., Weber, J., and Malik, J., (1994b) Robust Multiple Car Tracking with Occlusion Reasoning, *ECCV94*, pp A:189-196.

Kühne, R., Immes, S., (1993) Freeway Control Systems for Using Section-Related Traffic Variable Detection, *Pacific Rim TransTech Conference Proc., Vol 1*, ASCE, pp 56-62.

Kühne, R., Palen, J., Gardner, C., Ritchie, S., (1997) Section-Related Measures of Traffic System Performance, paper presented at the 76th annual TRB meeting, Transportation Research Board.

Larson, J., Van Katwyk, K., Liu, C., Cheng, H., Shaw, B., Palen, J., (1998) *A Real-Time Laser-Based Prototype Detection System for Measurement of Delineations of Moving Vehicles*. UCB-ITS-PWP-98-20, PATH, University of California, Berkeley, CA, 1998.

Levine, S., McCasland W., (1994) Monitoring Freeway Traffic Conditions with Automatic Vehicle Identification Systems, *ITE Journal*, Vol 64, No 3, pp 23-28.

Lin, W., Daganzo, C., (1997) A Simple Detection Scheme for Delay-Inducing Freeway Incidents, *Transportation Research-Part A*, Vol 31A, No 2, pp 141-155.

MacCarley, C. A., (1998) *Videobased Vehicle Signature Analysis and Tracking Phase 1: Verification of Concept and Preliminary Testing*. UCB-ITS-PWP-98-10, PATH, University of California, Berkeley, CA.

Petty, K., (1995) *Freeway Service Patrol (FSP): 1.1 The Analysis Software for the FSP Project*, PATH Research Report UCB-ITS-PRR-95-20, University of California, Berkeley.

Petty, K., Bickel, P., Ostland, M., Rice, J., Schoenberg, F., Jiang, J., Ritov, Y., (1997) Accurate Estimation of Travel Times From Single Loop Detectors, *Transportation Research-Part A*, Vol 32, No 1, pp 1-17.

Petty, K., Kwon, J., Ostland, M., Rice, J., and Bickel, P., (1999) A New Methodology for Evaluating Incident Detection Algorithms, [submitted for publication].

Pfannerstill, E., (1984) A Pattern Recognition System for the Re-identification of Motor Vehicles, *Proc. 7th International Conference on Pattern Recognition*, Montreal, IEEE, New Jersey, pp 553-555.

Reijmers, J., (1979) On-Line Vehicle Classification, *Proceedings of the International Symposium on Traffic Control Systems*, Vol 2B, Institute of Transportation Studies, University of California at Berkeley, pp 87-102.

Skabardonis, A., Noeimi, H., Petty, K., et al., (1995) *Freeway Service Patrols Evaluation*, PATH Research Report UCB-ITS-PRR-95-5, University of California, Berkeley.

Skabardonis, A., Petty, K., Noeimi, H., Rydzewski, D. and Varaiya, P., (1996) I-880 Field Experiment: Data-Base Development and Incident Delay Estimation Procedures, *Transportation Research Record 1554*, TRB, pp 204-212.

Van Aerde, M., Hellinga, B., Yu, L., Rakha, H., (1993) Vehicle Probes as Real-Time ATMS Sources of Dynamic O-D and Travel Time Data, *Large Urban Systems- Proc. of the Advanced Traffic Management Conference*, FHWA, pp 207-230.

Westerman, M., Immers, L., (1992) A Method for Determining Real-Time Travel Times on Motorways, *Road Transport Informatics/Intelligent Vehicle Highways Systems*, ISATA, pp 221-228.

Westerman, M., Litjens, R., Linnartz, J., (1996) *Integration of Probe Vehicle and Induction Loop Data- Estimation of Travel Times and Automatic Incident Detection*. PATH, University of California at Berkeley.

Windover, J., (1998) *Empirical Studies of the Dynamic Features of Freeway Traffic*, Dissertation, University of California.